

A SPECTROSCOPIC STUDY OF IONIC SOLVATION:
THE EFFECTS OF STERIC CROWDING AND
MATRIX FLUIDITY ON MATRIX
SOLVATION SPECTRA

By

MARK EDWIN FISHER

Bachelor of Science

Cameron University

Lawton, Oklahoma

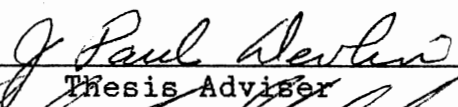
1985

Submitted to the Faculty of the
Graduate College of the
Oklahoma State University
in partial fulfillment of
the requirements for
the degree of
MASTER OF SCIENCE
July, 1989

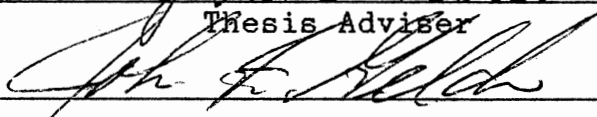
Thesis
1989
F535s
cop. 2

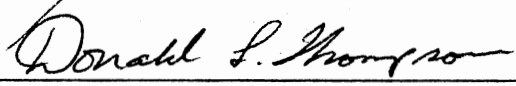
A SPECTROSCOPIC STUDY OF IONIC SOLVATION:
THE EFFECTS OF STERIC CROWDING AND
MATRIX FLUIDITY ON MATRIX
SOLVATION SPECTRA

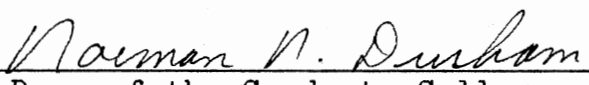
Thesis Approved:



Thesis Adviser







Dean of the Graduate College

ACKNOWLEDGMENTS

This work would have been impossible without the assistance of several important individuals. I would like to take this opportunity to thank them for their assistance.

I wish to thank Dr. J. Paul Devlin, my research adviser. Without your advice, patience, and guidance this work could not have been completed.

I wish to thank Dr. Donald Thompson and Dr. John Gelder for taking the time to serve on my committee.

The financial support of the National Science Foundation and Oklahoma State University are gratefully acknowledged.

I wish to thank the following for their friendship and helpful discussions: Gary Ritzhaupt, Robert Wooldridge, and Fouad Fleyfel, members of Dr. Devlin's research group; Kailash Swarna, Jeff Fuson, and Linda Mannsker, fellow graduate students.

Finally, I wish to dedicate this work to the members of my family for their faith, love, support, and endless encouragement. Without you, this work would have been impossible.

TABLE OF CONTENTS

Chapter	Page
I. LITERATURE REVIEW	1
Introduction	1
The Composition of the Vapors of Molten Alkali-Metal Nitrates	3
Matrix Isolation	4
The Nitrate Ion as a Structural Probe in Solutions	4
The Coordination Geometry of Alkali-Metal Oxyanion Contact Ion Pairs	7
The Effects of Solvation on Cation-Anion Interaction	10
The Effects of Anion Solvation on Matrix Spectra	14
Matrix Fluidity	15
Review of Matrix Solvation Data for $(\text{H}_2\text{O})_n \cdot \text{M} + \text{NO}_3^-$	16
II. EXPERIMENTAL	19
A Brief Outline of Sample Preparation.	19
A Description of the Sample Cells.	20
Preparation of Molecular Beams	31
Experimental Parameters.	34
Collection of Spectra.	37
III. EXPERIMENTAL RESULTS AND DISCUSSION	38
Results for t-Butanol as Solvent	38
Results for Water as Solvent	54
Summary.	61
REFERENCES	64

LIST OF TABLES

Table	Page
1. Free Nitrate Ion Selection Rules	5
2. A List of Hardware for the Glass Cell Depicted in Figure 2	22
3. A List of Hardware for the Metal Cell Depicted in Figure 3	25
4. A List of Hardware for the Oven Assemblies Depicted in Figure 4.	28
5. A List of Hardware for the Window Assemblies Depicted in Figure 5.	30
6. Estimated Maximum Annealing and Rigid Temperatures for Matrix Materials.	36
7. Approximate Band Positions for the Spectra in Figure 2.	42
8. Frequency Assignments and Maximum Splittings for the Cation Solvates of the Lithium Nitrate Ion Pair Solvated by t-Butanol, and a Comparison with the Splittings for THF and H ₂ O	43
9. A Comparison of the Change in Splitting of ν_3 for Each Solvation Step in the Solvation of Lithium Nitrate Ion Pairs by t-Butanol, THF, and H ₂ O.	43

LIST OF FIGURES

Figure	Page
1. Possible Coordination Geometries for a Li+NO ₃ ⁻ Ion Pair	9
2. A Sketch of the Low-Temperature Glass Infrared Spectroscopic Cell Cooled by Cryofluids	21
3. A Sketch of the Low-Temperature Metal Infrared Cell Cooled by a Closed-Cycle Helium Refrigerator.	24
4. A Sketch of the Oven Assemblies	27
5. A Sketch of the Window Assemblies	29
6. A Sketch Illustrating Substrate Orientation for Deposition and Collection of Spectra.	32
7. Infrared Difference Spectra of Lithium Nitrate Ion Pair Solvates with t-Butanol as the Solvent, Isolated in an Argon Matrix.	39
8. Matrix Spectra of t-Butanol Isolated in Argon	40
9. Infrared Spectra of 90 K Deposits of K+NO ₃ ⁻ and Li+NO ₃ ⁻ in Pure t-Butanol	46
10. Infrared Spectra of 90 K Deposits of K+NO ₃ ⁻ and Li+NO ₃ ⁻ in Pure t-Butanol after Annealing to 160 K	47
11. The Effect of Deposition Temperature and Annealing on the Infrared Spectra of the Solvates of Li+NO ₃ ⁻ Matrix Isolated in Pure t-Butanol	50
12. The Effect of Annealing on the Matrix Spectra of Li+NO ₃ ⁻ Ion Pairs Isolated in Pure t-Butanol.	51
13. A Comparison of Minimum Temperature Deposits of Li+NO ₃ ⁻ Ion Pairs in Pure Water and Pure t-Butanol	53

Figure	Page
14. The Effect of Deposition Temperature on the Matrix-Hydration Spectra of Li^+NO_3^- Ion Pairs in Pure Water Matrices.	56
15. The Effect of a Change in Cation on the Matrix Hydration Spectra of Alkali-Metal Nitrate Ion Pairs in Pure Water Matrices.	58

CHAPTER I

LITERATURE REVIEW

Introduction

The determination of the details of ionic solvation processes has been an important, yet elusive goal of researchers in the area of solution chemistry for many years. Early efforts at obtaining these details were primarily through the study of bulk electrolytic solutions (1) (2) and, although informative, the complex nature of bulk solutions make it difficult to gain a greater insight into the details of ionic solvation process at the molecular level. Workers have more recently focused on the behavior of the individual components present in electrolytic solutions, an approach which has provided insight into the details needed to form a more complete picture of the ionic solvation process.

Of particular interest in this study are the details concerning the solvation of strong electrolytes. In such a system, the electrostatic interaction between the ions in the solution is important. Theories which assume complete dissociation of an electrolyte in solution, such as the sphere-in-a-continuum model proposed by Debye and Huckel (3), do not adequately predict the behavior of these

solutions except at high levels of dilution where the ions are separated by several layers of solvent molecules. If two oppositely charged ions approach each other so that their primary solvation shells touch, the ions can no longer be treated as separate entities. This association between the ions results in what is commonly referred to as an "ion pair". The concept of ion pairing is frequently used to explain the deviations between observed behavior and the behavior predicted by models assuming complete dissociation in solutions of strong electrolytes (4).

In a solution of a strong electrolyte, intra- and intermolecular interactions both play critical roles in the dynamics of the solution. These interactions can be studied using vibrational spectroscopy (5). From spectral data, information which is important in the understanding of the solvation process can be obtained. These data include information such as solvation numbers (6) (7), the coordination geometry of ion pairs (8) (9), the nature and strength of solvent-ion interactions (10) (11) (12), and the identification of the various species present in a solution (13) (14).

Spectroscopic studies of the solvates of alkali-metal oxyanion ion pairs of the form $S_n \cdot M^+XO_m^-$ isolated in low-temperature inert gas matrices is one method that has yielded unique insights into the ion solvation process. Using matrix isolation techniques and vibrational spectroscopy, it is possible to observe the solvation of

neutral ion pairs, a process which has not been observed by other means. This data can be extremely useful in the interpretation of the liquid-solution spectra of electrolytes (15). In this study, the matrix-isolated contact ion pair solvates $S_n \cdot Li^+NO_3^-$, $S_n \cdot K^+NO_3^-$, and $S_n \cdot Rb^+NO_3^-$, where S is either water or t-butanol, are investigated.

The Composition of the Vapors of Molten Alkali-Metal Nitrates

It has been shown that the vapors of the alkali-metal halides and hydroxides, which are usually considered to be ionic, tend to form dimers and higher polymers (16). Mass spectroscopic studies performed by Buchler and Stauffer (17) indicate that polymers are also present in the vapors of $LiNO_3$ and $NaNO_3$. Their results indicate, along with decomposition products, a significant concentration of the dimers $Li_2(NO_3)_2$ and $Na_2(NO_3)_2$ and the monomers $LiNO_3$ and $NaNO_3$. Work done by Smith, James, and Devlin (18) supports this finding. Smith, et al., were able to isolate in inert gas matrices at low temperatures the molecules present in beams of salt vapors formed by heating metal nitrate salts *in vacuo* to approximately 50°C above their melting points. The infrared and Raman spectra of these matrix-isolated vapors indicate that the dominant species in these vapors is the monomer ion pair, $M^+NO_3^-$, with a small amount of the dimer.

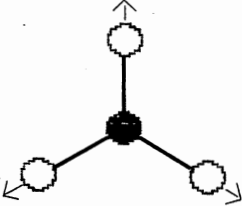
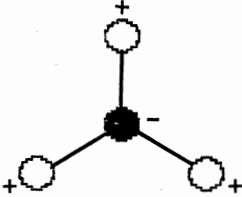
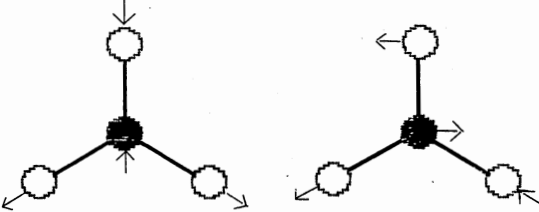
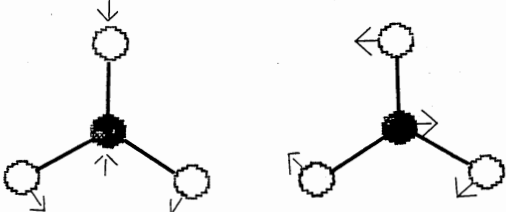
Matrix Isolation

The fact that the alkali-metal nitrates vaporize largely as ion pairs, and that these ion pairs can be isolated in an inert gas matrix (18), is important from the standpoint that ion-pair solvation studies can be performed using these matrix-isolated ion pairs as a probe into the solvation process. Using matrix isolation techniques (19), it is possible to isolate ion pairs in a matrix of inert gas containing a known concentration of a given solvent. By carefully regulating experimental conditions, it is possible to introduce solvent molecules into the solvation sphere of the cation in a controlled, stepwise manner so that the various solvates of the ion pair can be prepared and studied spectroscopically (15).

The Nitrate Ion as a Structural Probe in Solutions

An unperturbed nitrate ion of D_{3h} symmetry has six fundamental vibrational modes (4). As can be seen from Table 1, three of these modes should be infrared active, and three modes should be Raman active. Assuming that the C_3 rotational axis of the anion is maintained, ν_3 and ν_4 are both doubly degenerate. The degeneracy of these modes will be lost and each of the modes will be split into two modes of different frequency if the three-fold axis of symmetry of the nitrate ion is lost due to any symmetry-lowering

TABLE 1
FREE NITRATE ION SELECTION RULES

Mode	Description	Activity	Frequency cm ⁻¹
$\nu_1(A_1')$	symmetric stretch	R	1050
			
$\nu_2(A_2'')$	out of plane bend	I	825
			
$\nu_3(E')$	antisymmetric stretch	R, I	1384
			
$\nu_4(E'')$	planar bend	R, I	720
			

distortion of the anion. Janz (20) noted that environmental effects present in condensed states (solid and liquid) are frequently sufficient to cause the splitting of degenerate nitrate modes. It has since been shown that the splitting of the $\nu_3(E')$ anti-symmetric stretching mode of the nitrate anion is a useful tool in the elucidation of the structures of molten salts and concentrated aqueous solutions. It is this splitting that is the basis for much of the research dealing with solvation in oxyanion systems, and is essential to the present study.

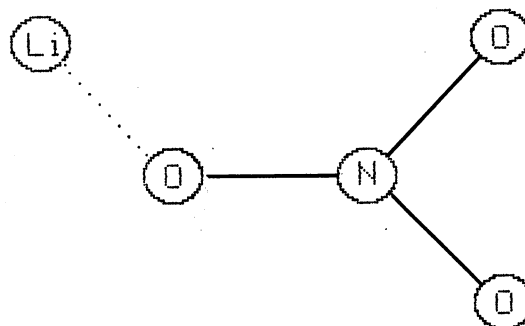
It has been established that the magnitude of the splitting of $\nu_3(E')$ is a sensitive measure of the degree of distortion of the nitrate ion by a contacting cation (10) (21). Furthermore, it has been shown that as the cation is solvated in a stepwise manner, a discontinuous collapse in the $\nu_3(E')$ splitting is observed (7). This reduction in the splitting of ν_3 has been attributed to two effects. The first, which is the more significant of the two in the initial stages of solvation, is the reduction of the ability of the cation to polarize the anion due to a transfer of electron density from the solvent molecules, which are Lewis bases, to the cation (7). The second effect is a disruption of the bonding between the cation and the anion due to steric crowding as an increasing number of solvent molecules are introduced into the solvation sphere of the cation (22). These two effects will be discussed in more detail later in this chapter.

The Coordination Geometry of Alkali-
Metal Oxyanion Contact Ion Pairs

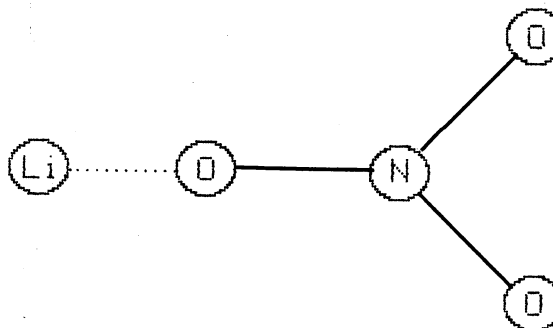
It has been shown that the preferred coordination geometry for a variety of oxyanion alkali-metal ion pairs is usually bidentate in nature (8 - 10) (23 - 24). Normal mode calculations performed by Hester and co-workers (26) (27) show that, at least in principle, it is possible to distinguish between monodentate and bidentate binding if the symmetries of the N-O stretching modes can be assigned. Their work predicts that for either denticity, the two highest frequency N-O modes ($A_1 + B_2$) are due to the splitting of the components of the D_{3h} E' antisymmetric stretching mode of free nitrate due to polarization of the nitrate ion by the cation. For the bidentate case, the symmetric A_1 mode moves to higher frequency, while the B_2 mode moves to lower frequency. For the monodentate case, the reverse situation is observed, with the antisymmetric B_2 component moving to higher frequency, and the A_1 mode moving to lower frequency. Both modes are infrared and Raman active. Since the A_1 mode is symmetric, it should exhibit Raman polarization, while the antisymmetric B_2 mode should exhibit Raman depolarization (28). Hence, a careful Raman depolarization study should enable the denticity of the ion pair to be determined. Unfortunately, Raman depolarization ratios are difficult to obtain for matrix-isolated samples. For perchlorate ion pairs, the situation is simplified

somewhat. Devlin and co-workers (24) were able to show that matrix-isolated alkali-metal perchlorate ion pairs favored a bidentate-like geometry based on the fact that the singlet near 1100 cm^{-1} assigned to the triply degenerate $\nu_3(f)$ mode for an unperturbed free perchlorate ion was split into three bands in the ion-pair spectrum. This finding is consistent only if the tetrahedral symmetry of the free perchlorate ion is lowered to C_{2v} or lower through a bidentate interaction with the cation. C_{3v} symmetry, consistent with monodentate binding, would split $\nu_3(f)$ into only two components. Of interest was the finding that the spacing between ν_{3a} and ν_{3b} for matrix-isolated nitrate ion pairs and the spacing between ν_{3a} and ν_{3c} for matrix-isolated perchlorate ion pairs is quite similar. This finding led to the reexamination of the coordination geometry of nitrate ion pairs, which had originally been thought to be monodentate. Devlin and Moore (10) performed *ab initio* LCAO-MO-SCF molecular orbital calculations for the Li^+NO_3^- ion pair. The results of these calculations predict that the minimum energy structure is a planar bidentate structure of C_{2v} symmetry (structure C of Figure 1), and that it is 28 kcal/mole more stable than the C_{2v} monodentate structure (structure B of Figure 1), which is calculated to be the minimum energy monodentate structure. The C_s monodentate structure (structure A of Figure 1), which was suggested by early electron diffraction measurements (29), was found to be less stable than the C_{2v} monodentate structure by

A. C_s Monodentate



B. C_{2v} Monodentate



C. C_{2v} Bidentate

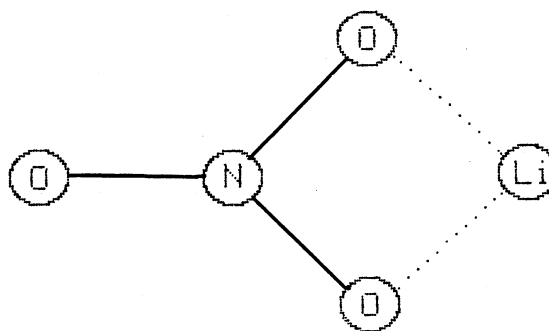


Figure 1. Possible Coordination Geometries for a Li^+NO_3^- Ion Pair.

3.1 kcal/mole. In addition, Beattie and co-workers (8) were able to show by using isotope frequency and intensity patterns that ^{18}O enriched matrix-isolated KNO_3 exhibits bidentate coordination. These studies firmly establish that the coordination geometry of matrix-isolated alkali-metal ion pairs is usually bidentate in nature.

The Effects of Solvation on Cation-Anion Interaction

High-pressure mass spectroscopic studies (30) of the thermochemical properties of gas phase cluster ions formed by the solvation of Li^+ and Na^+ with NH_3 reveal that the interaction between solvent and cation is greatest for the first step of solvation and decreases for each subsequent solvation step until the ion is completely solvated. This effect is predicted by the SCF calculation performed by Devlin and Moore (10) on hydrated Li^+NO_3^- ion pairs, as the charge on the Li^+ cation is shown to decrease asymptotically with each solvation step as the cation charge becomes more diffuse due to charge cancellation through transfer of electron density from the solvent (a Lewis base) to the cation (a Lewis acid). This charge cancellation results in a decrease in the ability of the cation to perturb the nitrate ion, resulting in a decrease in the magnitude of the splitting of ν_3 . Thus, if charge cancellation is largely responsible for the collapse in the splitting of ν_3 , then the collapse in ν_3 should be greatest in magnitude for the

first solvation step, with the magnitude in the collapse of ν_3 becoming progressively smaller with each added solvent molecule. Early matrix solvation experiments (31) seemed to support this hypothesis, as the collapse in the splitting of ν_3 was observed to be largest for the first stage of solvation, followed by progressively smaller collapse step sizes until the splitting approached that of the ion pair in the pure solvent. However, improved matrix spectra obtained through the use of more modern instrumentation and over a wider range of experimental conditions revealed that the early matrix spectra, although qualitatively useful, were somewhat misleading in a quantitative sense. It is now known that the collapse step sizes are normally of similar magnitude for each of the solvation steps or, depending on the choice of solvent, tend to increase somewhat (7) (22). Since the charge neutralization effect decreases for each solvation step, another factor must work in concert with charge neutralization to produce changes in splitting of similar or increased magnitude for each solvation step.

As an ion pair is solvated, an increasing amount of steric repulsion between the anion and the solvent molecules in the inner coordination sphere of the cation occurs. These repulsive forces tend to push the cation and anion apart resulting in a substantial decrease in the interaction between the two ions and a corresponding collapse in the splitting of ν_3 . For the first solvation step the steric effect is minimal, but will increase for each solvation step

as the cation is solvated (22). Thus, as the degree of solvation progresses the steric factor increases while the charge neutralization factor decreases. It has been proposed (7) (22) that the overall effect can then be viewed as a combination of the steric and charge neutralization factors, resulting in a relatively constant step size in the collapse of ν_3 .

As an increasing number of solvent molecules are introduced into the inner coordination sphere of the cation, it seems plausible that a switch from bidentate to monodentate binding between the cation and anion might occur at some stage. Such a change would create more space for the solvent molecules resulting in a lower energy configuration due to a decrease in repulsive forces between the anion and the solvent molecules within the inner coordination sphere of the cation. The observation of changes in denticity have been anticipated for quite some time, but have been difficult to document experimentally.

As previously mentioned, the normal mode calculations of Hester (26) indicate that for bidentate binding ν_{3a} (the symmetric A_1 component of ν_3) lies at a higher frequency than ν_{3b} (the anti-symmetric B_2 component of ν_3), and for monodentate binding the situation is reversed with ν_{3b} at higher frequency than ν_{3a} . In the monodentate case ν_{3a} lies closer to the nitrate ν_1 symmetric stretching mode than does ν_{3b} giving rise to a possible ν_1 - ν_{3a} resonant interaction which should shift ν_{3a} to higher frequency (22). This shift

in ν_{3a} to higher frequency would place it closer to the position of ν_{3b} resulting in a decrease in the magnitude of the splitting of ν_3 . Thus, the magnitude of the splitting of ν_3 for a particular solvate exhibiting monodentate binding will be smaller than for the same solvate exhibiting bidentate binding. Hence, a change from bidentate to monodentate binding could result in an unusually large decrease in the splitting of the nitrate ν_3 mode for the solvation step in which the change in binding occurs. Large solvation steps have been observed experimentally, but the results were inconclusive as to whether a change in binding was responsible for the large step size. Of note are the large solvation steps that have been reported for the two-solvate to three-solvate step for Li^+NO_3^- isolated in argon matrices containing the solvents N,N-dimethylformamide (DMF) or tetrahydrofuran (THF) (7).

In addition, a study of Raman depolarization ratios could theoretically be used to determine if a change in denticity has occurred, but as previously noted, these ratios are difficult to obtain for matrix isolated samples. In liquid solutions, Raman depolarization ratios have been obtained, and indicate a change from bidentate to monodentate binding for the fourth solvation step for contact-paired Li^+NO_3^- in dimethylsulfoxide (DMSO) solutions (13), and for the third step in a DMF solution (32). Part of the research for this thesis focuses on an attempt to experimentally induce and observe steric effects through

a study of the matrix solvates of Li^+NO_3^- and t-butyl alcohol (TBA). TBA is the largest commercially available deuterated solvent molecule and was chosen for this study in hopes that it would produce exceptionally large steric effects which could be readily observed in the matrix spectra.

The Effects of Anion Solvation on Matrix Spectra

The formation of cation solvates normally dominate over the formation of anion solvates in matrices due to the fact that the cation solvates are preferred energetically (22). A degree of anion solvation does occur, however, and in some cases can have a significant effect on matrix solvation spectra. In matrices exhibiting high solvent dilution (typically 1% solvent or less), the band pair components corresponding to the lower ion-pair solvates are typically sharp, resembling the band pair components for bare (unsolvated) ion pairs. However, in matrices with higher solvent concentrations (a condition necessary to favor the formation of the higher solvates), the bands corresponding to a given solvate are usually a factor of two to four broader than the corresponding bands in matrices containing less solvent, and also exhibit a shift of approximately 5 cm^{-1} . This broadening and shifting is attributed to anion solvation (22). Band broadening due to anion solvation can reduce the usefulness of matrix-solvation spectra in that it

sometimes limits the degree of accuracy with which solvate band positions can be located, making quantitative judgments of the data difficult. For $M^+NO_3^-$ ion pairs, the ν_{3a} component of ν_3 is more sensitive to solvation effects than the ν_{3b} component, so the effects of anion solvation are much more pronounced and hence more troublesome when dealing with the ν_{3a} component (22).

Anion solvation can limit the usefulness of matrix solvation data for other reasons as well. For example, water strongly hydrogen bonds with the nitrate ion in pure water matrices producing a distortion that lifts the degeneracy of the nitrate ν_3 mode and results in a splitting of approximately 50 cm^{-1} for this band (31), making it impossible to observe spectroscopically any of the ion pair hydrates with a splitting of less than 50 cm^{-1} .

Matrix Fluidity

For inert gas matrices containing low concentrations of solvent molecules, the statistically most probable environment for the ion pair should be a configuration in which the ion pair is surrounded by matrix molecules (31). This is not what is observed experimentally, since for $Li^+NO_3^-$ ion pairs isolated at a temperature of 12K in argon matrices containing only 1% H_2O , the first two ion pair solvates are clearly visible in the spectrum along with the bare ion pair (7). This implies that as the matrix forms at 12K, a certain amount of fluidity is present at the growing

surface of the matrix, enabling some of the solvent molecules to encounter ion pairs. It is also conceivable that if the matrix contains a dissociating solvent, a degree of solvent insertion could occur before the matrix becomes rigid, resulting in the formation of solvent-separated ion pairs as the matrix forms.

Review of Matrix Solvation

Data for $(\text{H}_2\text{O})_n \cdot \text{M} + \text{NO}_3^-$

The use of water as a solvent in matrix solvation experiments presents several difficulties not normally encountered in matrix solvation studies. Already discussed is the fact that water strongly hydrogen bonds with the nitrate ion in pure water matrices, which is a serious limitation in that it may prevent the observation of the complete set of ion pair hydrates (33). In addition, water is a dissociating solvent for inorganic salts, resulting in the question as to whether or not ion pairs retain their contact nature when isolated in a pure water matrix (7) (34).

Given that water is a dissociating solvent and that there is a certain amount of fluidity present at the surface of a matrix during deposition and throughout the matrix upon annealing, it is possible that solvent-separated ion pairs could form. For matrix-isolated $\text{Li} + \text{NO}_3^-$, five distinct hydrates are seen in the matrix spectrum. It is possible that the fifth step of hydration results in a solvent-

separated ion pair rather than the pentahydrate of the contact ion pair (7). Matrix solvation data indicate that solvent insertion does not occur for Li^+NO_3^- in the nondissociating solvents acetonitrile (ACN), tetrahydrofuran (THF), glyme, N,N-dimethylformamide (DMF), or pyridene (6) (7) (22). There is also evidence that Li^+NO_3^- remains contact-paired under low-temperature matrix conditions in the dissociating solvent dimethylsulfoxide (DMSO). The liquid DMSO solution spectrum exhibits a single band for ν_3 which has been assigned to solvent-separated ions (35). The matrix spectrum reveals a splitting in ν_3 of 59 cm^{-1} for the maximum solvate, $(\text{DMSO})_4\cdot\text{Li}^+\text{NO}_3^-$, in a 100% DMSO matrix (6). It is unlikely that this splitting is due to anion-solvent interaction since no splitting of ν_3 was observed for solvent-separated ions in the liquid spectrum. The splitting must then be due to distortion of the anion by the cation, indicating cation-anion contact is retained under matrix conditions. Although anion-solvent interaction in 100% water matrices may eliminate the observation of any hydrates producing splittings of less than 50 cm^{-1} , there is a measure of cation dependence in the splitting and positioning of the bands assigned to the highest observable hydrates in these spectra. The splitting for the highest observable hydrate when the cation is Li^+ is 65 cm^{-1} , with the value falling to approximately 50 cm^{-1} when K^+ is the cation (21). This cation-dependence in the splitting of ν_3 has been cited as evidence for contact pairing in water

matrices (7).

Dilute aqueous alkali metal nitrate and perchlorate liquid solutions, which should consist largely of completely solvated (free) ions, have been vitrified by the rapid cooling of aerosol droplets of these solutions onto a solid cryoplate and then investigated spectroscopically. Mayer (34) concluded that for lithium and sodium nitrate, contact ion paired hydrates are formed upon vitrification of the aqueous solution of ions, while vitrified potassium and rubidium nitrate result in solvent-separated ion pairs. The formation of ion pairs in the lithium and sodium nitrate solutions upon rapid quenching at low temperatures is surprising in that it has been concluded that ion pairing is favored by an increase in temperature for solutions of LiNO_3 in water (36) and in DMSO (13).

Mayer's results are particularly interesting in that a striking degree of similarity exists between these spectra and the matrix solvation spectra. These similarities imply that the nature of the species trapped from the aqueous liquid solutions used for aerosol formation by Mayer must change considerably as they are being quenched on the cryoplate. Part of the work done for this thesis involves a comparison of the nitrate ν_3 bands for matrix samples prepared at 12 K with those prepared at 90 K in an effort to determine the effects of variable matrix fluidity on the ionic species trapped from the vapor phase.

CHAPTER II

EXPERIMENTAL

A Brief Outline of Sample Preparation

The ion-pair solvates studied in this work were prepared using typical matrix-isolation techniques. These techniques have been discussed at length (19), so a brief outline of the technique will be presented here. In general, matrix-isolation experiments consist of simultaneously condensing onto a cryogenically cooled substrate the vapors of an inert matrix material along with the vapors of one or more reactive or unstable species in a manner such that the reactive / unstable specie or species are isolated from each other within the inert matrix. Since diffusion can usually be controlled within the matrix, the reactive or unstable species are effectively trapped within the matrix and can be held there indefinitely. A common type of matrix study involves isolating two or more highly reactive species from each other within a matrix. Controlled diffusion is then allowed within the matrix, enabling the reactive species to seek out and react with each other at a rate slow enough to enable studies which could not normally be performed if the reaction were allowed to proceed under normal conditions. In this study, ion-pair

solvates were prepared and studied spectroscopically using a similar type of experiment. Alkali-metal nitrate ion pairs were isolated in inert-gas matrices containing varying concentrations of a solvent, or in some cases matrices of pure solvent. The matrix was then annealed at a temperature high enough to allow controlled diffusion within the matrix, enabling the solvent molecules to interact with the ion-pairs and form the various ion-pair solvates which were then studied spectroscopically.

A Description of the Sample Cells

Since this work was done at very low temperatures, it was necessary to thermally isolate the sample from the surroundings. This was accomplished by preparing the samples in standard low-temperature spectroscopic sample cells under high-vacuum conditions (typically 10^{-6} torr). The sample cell was attached to a high-vacuum system during sample deposition, and was designed so the entire cell could be removed from the vacuum system after sample preparation and transferred to the spectrometer for collection of the spectra. Since the sample cell was not attached to the vacuum system during spectral collection, it was imperative that the cell be leak-proof in order to maintain a vacuum long enough to enable collection of the spectra.

Two different sample cells were used in this work. The first cell (Figure 2 and Table 2) was a standard low-temperature glass infrared spectroscopic cell cooled by

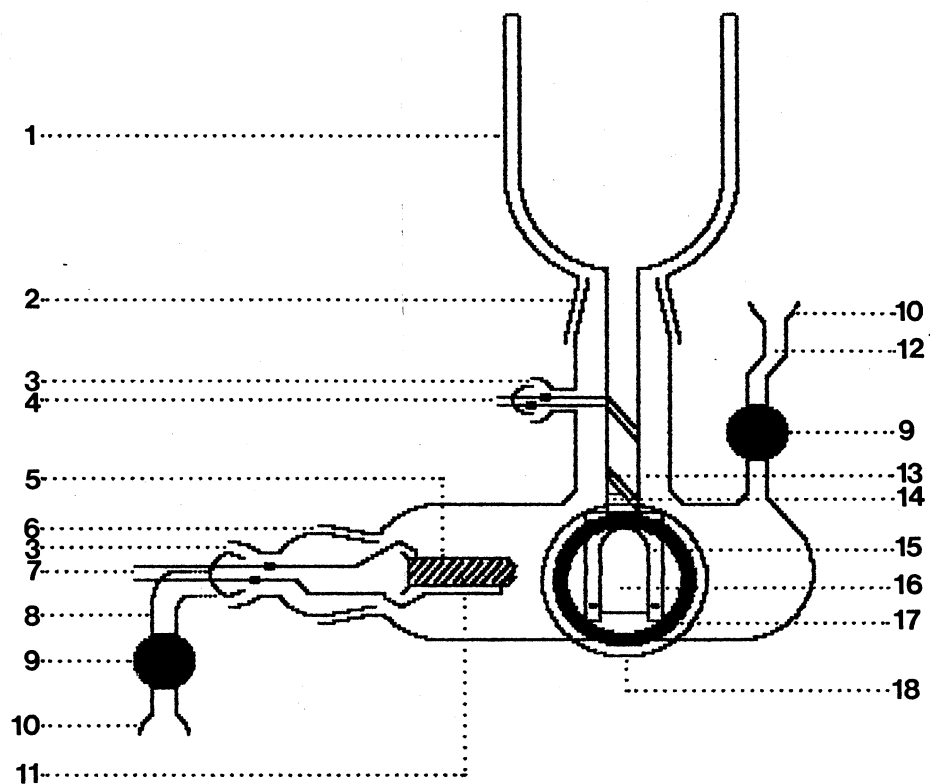


Figure 2. A Sketch of the Low-Temperature Glass Infrared Spectroscopic Cell Cooled by Cryofluids

TABLE 2
A LIST OF HARDWARE FOR THE GLASS
CELL DEPICTED IN FIGURE 2

Item Number	Description
1	Silvered Glass Dewar Flask
2	40/50 Glass Standard Taper Joint
3	28/12 Glass Ball-Socket O-ring Joint
4	Thermocouple Lead-Through Pins and Connectors
5	Oven Assembly
6	34/45 Glass Standard Taper Joint
7	Heater Lead-Through Pins and Connectors
8	Matrix Gas Inlet
9	Stopcock
10	18/9 Ground-Glass Socket
11	Nichrome Heating Element
12	Pump-Out Port
13	Iron-Constantan Thermocouple Leads
14	Kovar Seal
15	Window Assembly
16	CsI Sample Substrate
17	Ground-Glass Window Mounting Flange
18	KBr Outer Window

liquid nitrogen. This cell was used to prepare ion-pair solvates in pure solvent matrices at 90 K . The second cell (Figure 3 and Table 3), which was used to prepare ion-pair solvates isolated in argon matrices, was a standard metal infrared spectroscopic cell cooled by an Air Products CSA-202 closed-cycle helium refrigerator equipped with an Air Products APD-8 temperature controller.

Although the two cells are quite different in appearance, both contain essentially the same features. Over the outside portholes of each cell are two polished KBr spectroscopic windows that enable the infrared beam of the spectrometer to pass through the sample cell. Both contain a resistively-heated quartz Knudsen oven (Figure 4 and Table 4) that is used to generate a molecular beam of ion-pairs, and a delivery tube for the introduction of the matrix gas and / or solvent vapor. The delivery tube and oven are carefully aligned so that the molecular beams coming from each are coincident upon a cryogenically cooled CsI spectroscopic window at approximately the same point. This window is secured to a cryogenically-cooled cold stem by a clamping plate and screws, with indium gaskets on both sides of the window to insure good thermal contact (Figure 5 and Table 5). The cold stem is approximately centered between the outer KBr windows. The cells are designed so that the stem holding the CsI sample substrate can be rotated. During deposition, the substrate is oriented so that the molecular beams exiting from the oven and matrix gas

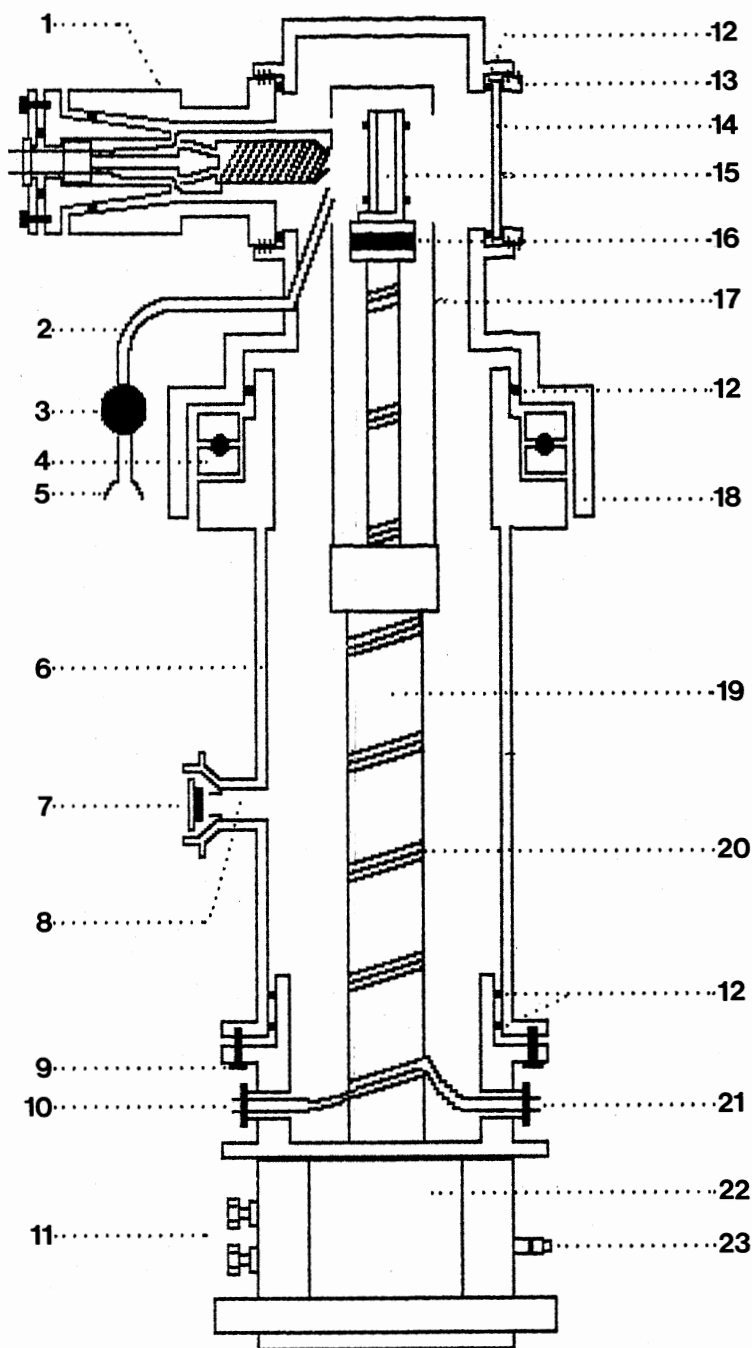


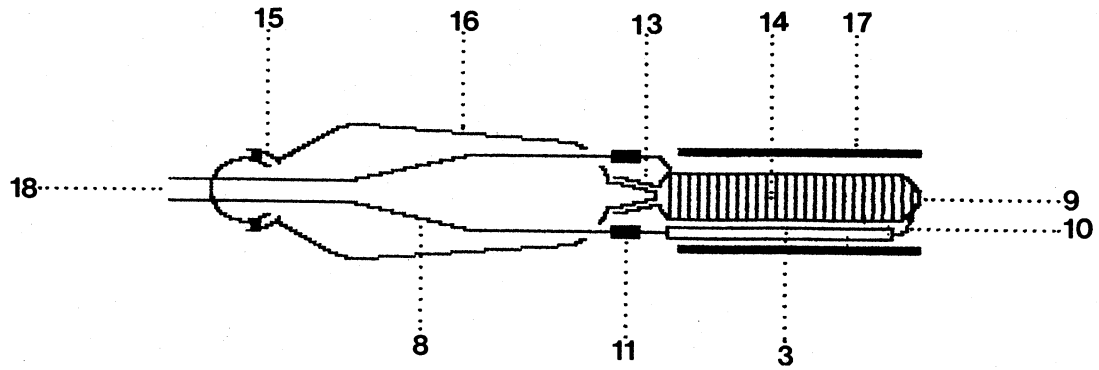
Figure 3. A Sketch of the Low-Temperature Metal Infrared Cell Cooled by a Closed-Cycle Helium Refrigerator

TABLE 3
A LIST OF HARDWARE FOR THE METAL CELL
DEPICTED IN FIGURE 3

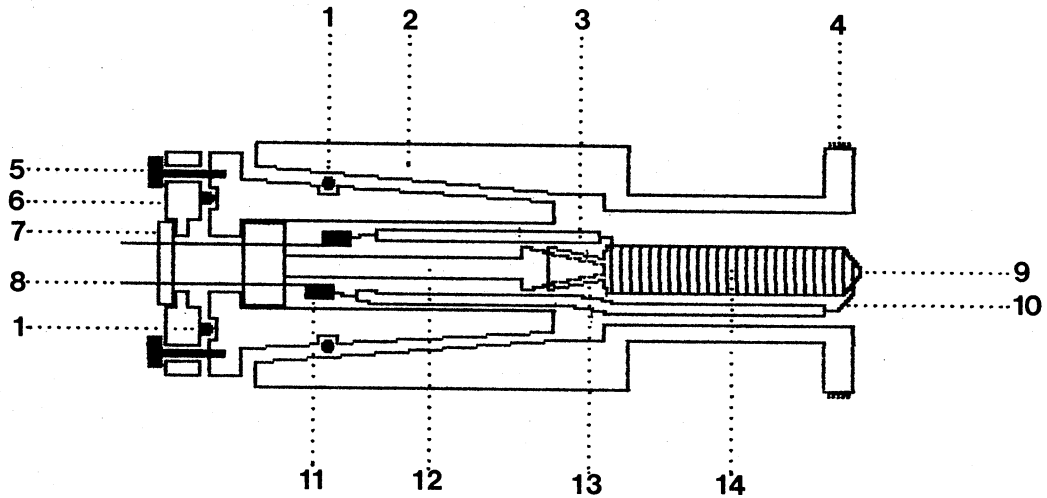
Item Number	Description
1	Oven Assembly
2	Matrix Gas Inlet
3	Stopcock
4	Bearing
5	18/9 Ground Glass Socket
6	Stainless Steel Vacuum Vessel
7	Richardson Valve
8	Pump-Out Port
9	Hex-Head Screw
10	Thermocouple Lead-Through
11	Helium Pressure Connectors
12	O-Ring Seals
13	Threaded Brass Window Fastener
14	KBr Outer Window
15	Window Assembly
16	Foil Heater
17	Radiation Shield
18	Rotatable Brass Vacuum Shroud
19	OFHC Copper Cold Stem
20	Thermocouple and Heater Leads
21	Heater Lead-Through
22	Displacer / Expander Assembly

TABLE 3 (Continued)

Item Number	Description
23	Power Connector



Oven Assembly from Glass Cell
(From Figure 2)

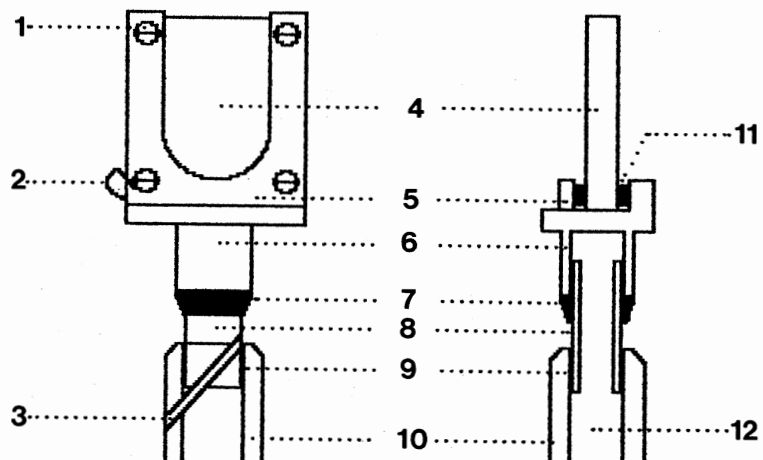


Oven Assembly from Metal Cell
(From Figure 3)

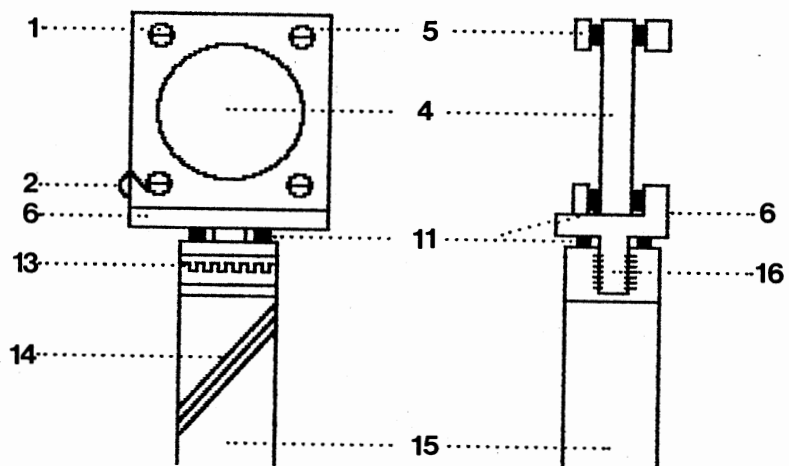
Figure 4. A Sketch of the Oven Assemblies

TABLE 4
A LIST OF HARDWARE FOR THE OVEN
ASSEMBLIES DEPICTED IN FIGURE 4

Item Number	Description
1	O-Ring Seal
2	29/42 Stainless Steel Standard Taper O-Ring Joint
3	Woven Glass Insulation
4	Threaded Mounting Flange
5	Hex-Head Screw
6	Stainless Steel End Plate
7	Ceramic Leadthrough
8	Copper Leads
9	Oven Orifice
10	Nichrome Wire Resistance Heater
11	Electrical Connectors
12	Glass Support Rod
13	7/25 Quartz Standard Taper Joint
14	Quartz Knudsen Oven
15	18/9 Glass Ball-Socket O-Ring Joint
16	34/45 Glass Standard Taper Joint
17	Aluminum Foil Covered Glass Radiation Shield
18	Heater Lead-Through



Window Assembly from Glass Cell
(From Figure 2)



Window Assembly from Metal Cell
(From Figure 3)

Figure 5. A Sketch of the Window Assemblies

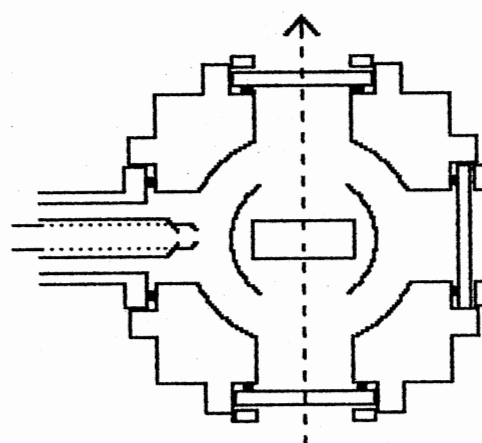
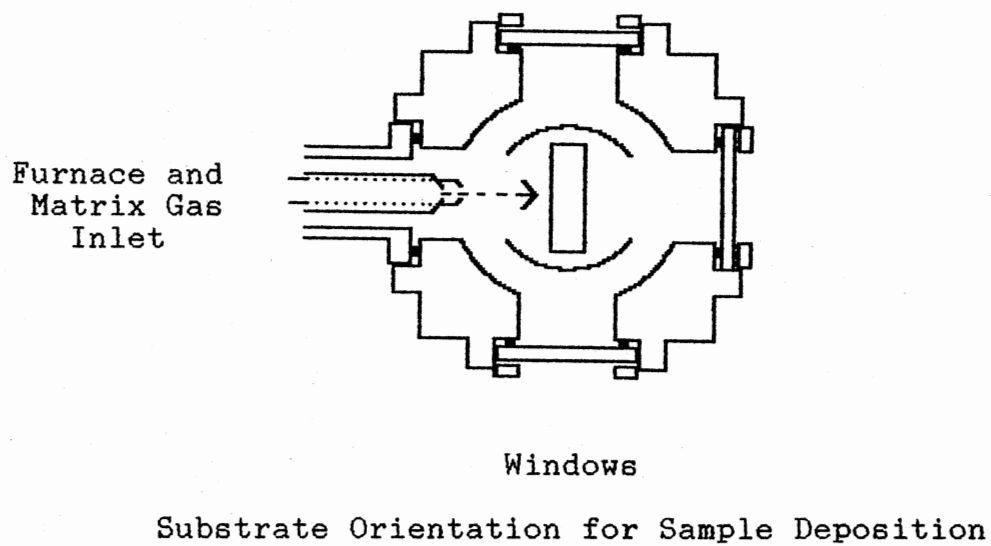
TABLE 5
A LIST OF HARDWARE FOR THE WINDOW
ASSEMBLIES DEPICTED IN FIGURE 5

Item Number	Description
1	Clamping Screw With Nut and Lock Washer
2	Thermocouple Mounting Junction
3	Iron / Constantan Thermocouple Leads
4	CsI Substrate
5	OFHC Copper Cover Plate
6	OFHC Copper Window Mounting Block
7	Silver Solder Joint
8	Kovar Sleeve
9	Glass / Kovar Seal
10	Glass Cold Stem
11	Indium Gaskets
12	Cryofluid Passage
13	Mylar / Foil Heater
14	Gold / Chromel Thermocouple leads and Heater Leads
15	OFHC Copper Cold Stem

delivery tube strike the face of the substrate (Figure 6). To enable the collection of spectra, the sample substrate must then be rotated approximately 90 degrees so that the face of the substrate is parallel to the outer windows enabling the spectrometer beam to pass through the sample. Substrate temperatures are monitored using an appropriate thermocouple attached between the copper mounting block and substrate. Finally, each cell has a pump-out port sealed by a stopcock. This port is located so that the cell can be easily attached to the vacuum system.

Preparation of Molecular Beams

The molecular beams of ion pairs were prepared from the vapors of the appropriate alkali-metal nitrate salt by heating the salt to a temperature slightly above its melting point in the appropriate oven assembly previously described (Figure 4 and Table 4). The oven temperature was controlled by varying the current supplied to the heater. Regulation of the current was accomplished by the use of two variacs connected in series. The first variac was used to limit the maximum current supplied to the heater in order to prevent heater burnout, and the second was used as a fine-adjustment to obtain the desired current setting. The temperature of the oven assembly could not be measured accurately, so the current setting required to produce a sample with an optimum ratio of ion pairs to matrix/solvent molecules was determined by trial and error. To limit the formation of



Substrate Orientation for Collection of Spectra

Figure 6. A Sketch Illustrating Substrate Orientation for Deposition and Collection of Spectra

decomposition products, the salts were dried prior to deposition by heating *in situ* under vacuum for several hours at a temperature slightly below the melting point of the salt. The salts used were LiNO_3 (Fisher Scientific), KNO_3 (Baker Analyzed Reagent), and RbNO_3 (Baker Analyzed Reagent).

The vapor beam of matrix gas and/or solvent vapor was generated in one of two ways. The simplest method, which was used to prepare samples of ion pairs isolated in pure solvent matrices at 90 K, was to form the beam directly from the vapors above the liquid solvent which was contained in a liquid reservoir at room temperature. The second method, which was used for the 12 K deposition of ion pairs in argon matrices containing solvent molecules, involved mixing the argon matrix gas and the desired solvent vapor in a 2-liter gas bulb prior to sample deposition. This was accomplished by loading into an evacuated gas bulb the solvent vapor at the solvent ambient vapor pressure, and then bleeding into the bulb enough argon to produce the desired ratio of argon-to-solvent for the experiment. This mixture was then used to form the vapor beam. During deposition, the flow rate of either the gas mixture or pure solvent vapor was monitored using a 1/16" Fischer-Porter glass flow meter in order to achieve the correct ratio of ion pairs to solvent/matrix molecules. Deuterated *t*-butanol, $(\text{CD}_3)_3\text{COD}$, (d-10, 99%, Stohler Isotopes) was chosen over $(\text{CH}_3)_3\text{COH}$ as a solvent because of the presence of fewer interfering bands in the

region of the nitrate vs antisymmetric stretching mode. The water used in this study was doubly-distilled and deionized. Both solvents were degassed by at least three freeze-pump-thaw cycles before use. The matrix gas used throughout was argon (99.98%, Union Carbide).

Experimental Parameters

The fact that diffusion occurs in matrices is desirable in that carefully controlled annealing of a matrix sample after deposition gives isolated ion pairs and solvent molecules within the matrix sufficient mobility to seek out and interact with each other, leading to the formation of the various ion-pair solvates of interest in this study. However, during sample deposition the goal is to isolate ion-pairs from solvent molecules within the matrix. Thus, diffusion during sample deposition is undesirable and must be kept to a minimum by carefully controlling experimental parameters.

During sample preparation, the sample substrate must be maintained at a temperature low enough to insure that the matrix remains rigid. In addition, an extremely rapid cooling rate is necessary to insure that the matrix becomes rigid as quickly as possible after condensation, hence limiting the amount of time that diffusion can occur (19).

An approximate guideline is that a matrix is usually considered rigid at temperatures below 30% of the melting point of the matrix material. Annealing of the matrix

commonly occurs at temperatures between 30% to 50% of the matrix melting point. At temperatures above 50% of the melting point of the matrix, the vapor pressure of the matrix typically becomes high enough that the matrix starts to evaporate, destroying the sample (19).

Table 6 summarizes approximate maximum rigid and annealing temperatures for the matrix materials used in this study. These temperatures are included as estimates and are based on the guidelines outlined in the preceding paragraph. Following these estimates, argon-isolated samples were prepared at approximately 12 K, and samples with pure (amorphous) solvent matrices of water or t-butanol were prepared at 85 K to 90 K. These temperatures are near or below the estimated maximum rigid temperatures for the matrix materials used and should insure that the matrices are fairly rigid when held at or below these temperatures. Some argon-isolated samples were annealed by holding at temperatures ranging from 20 K to 40 K for approximately 5 minutes. Water and t-butanol matrices were annealed at temperatures ranging from 110 K to 140 K. All annealed samples were re-cooled to deposition temperature before spectral collection.

It has already been mentioned that the heat released on condensing and cooling the matrix materials must be conducted away from the sample as rapidly as possible to limit diffusion. The high cooling rates necessary to achieve this can be obtained only if the matrix is deposited

Table 6

ESTIMATED MAXIMUM ANNEALING AND RIGID
TEMPERATURES FOR MATRIX MATERIALS

Matrix Material	Melting Point, Kelvin	Maximum Annealing Temperature, Kelvin	Maximum Rigid Temperature, Kelvin
Ar	84	42	25
H ₂ O, amorphous	273	137	82
(CD ₃) ₃ COD, amorphous	284	142	85

slowly. Thus, the flow rates of the matrix gasses were held at very low levels to insure that the heat released could be conducted away at a rate fast enough to prevent heating of the sample. With these small flow rates, sample deposition time ranged from two to six hours in order to obtain a sample of adequate thickness to study spectroscopically.

Collection of Spectra

Infrared spectra were collected using a Digilab FTS-20C vacuum spectrometer at 2 cm^{-1} resolution. Spectra consisted of 40-200 interferograms coadded and processed by a Data General Corporation Nova 3/12 computer with a fast-Fourier transform routine using double precision arithmetic.

CHAPTER III

EXPERIMENTAL RESULTS AND DISCUSSION

Results for t-Butanol as Solvent

The infrared difference spectra of the ion pair solvates of Li^+NO_3^- / t-butanol isolated in argon matrices are shown in Figure 7. The concentrations of t-butanol in the matrices and temperatures are as follows: spectrum (A), 1% at 9 K; spectrum (B), 4% at 14 K; spectrum (C), 12% at 12 K; spectrum (D), 12% annealed to 42 K; and spectrum (E), 100% annealed to 125 K. The numerals in the figure label the ν_3 doublets for each of the solvates, with the numerals indicating the number of solvent molecules per ion pair. The spectra in Figure 8 are of t-butanol isolated in argon matrices and were used to subtract the t-butanol bands from the original ion-pair solvate spectra resulting in the difference spectra shown in Figure 7. The percentages indicated in Figure 8 represent the percent t-butanol in the matrix. The t-butanol bands did not all subtract cleanly, so Figure 8 is included to facilitate the identification of matrix-isolated solvent bands still visible in the difference spectra of Figure 7. The peaks labeled with an asterisk in Figure 7 are assigned to matrix-isolated t-butanol. There are 4 clearly defined solvation stages

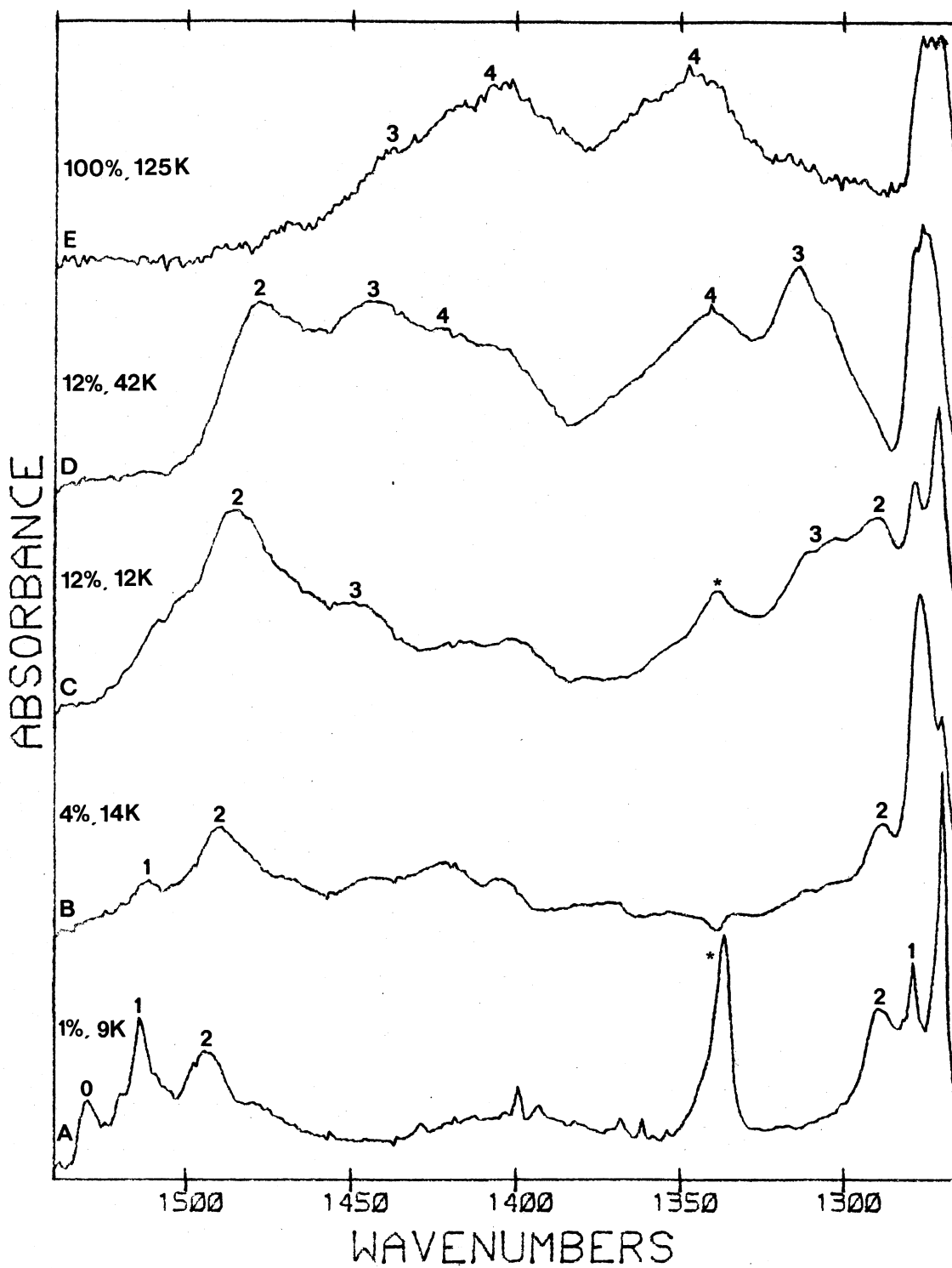


Figure 7. Infrared Difference Spectra of Lithium Nitrate Ion Pair Solvates with *t*-Butanol as the Solvent, Isolated in an Argon Matrix

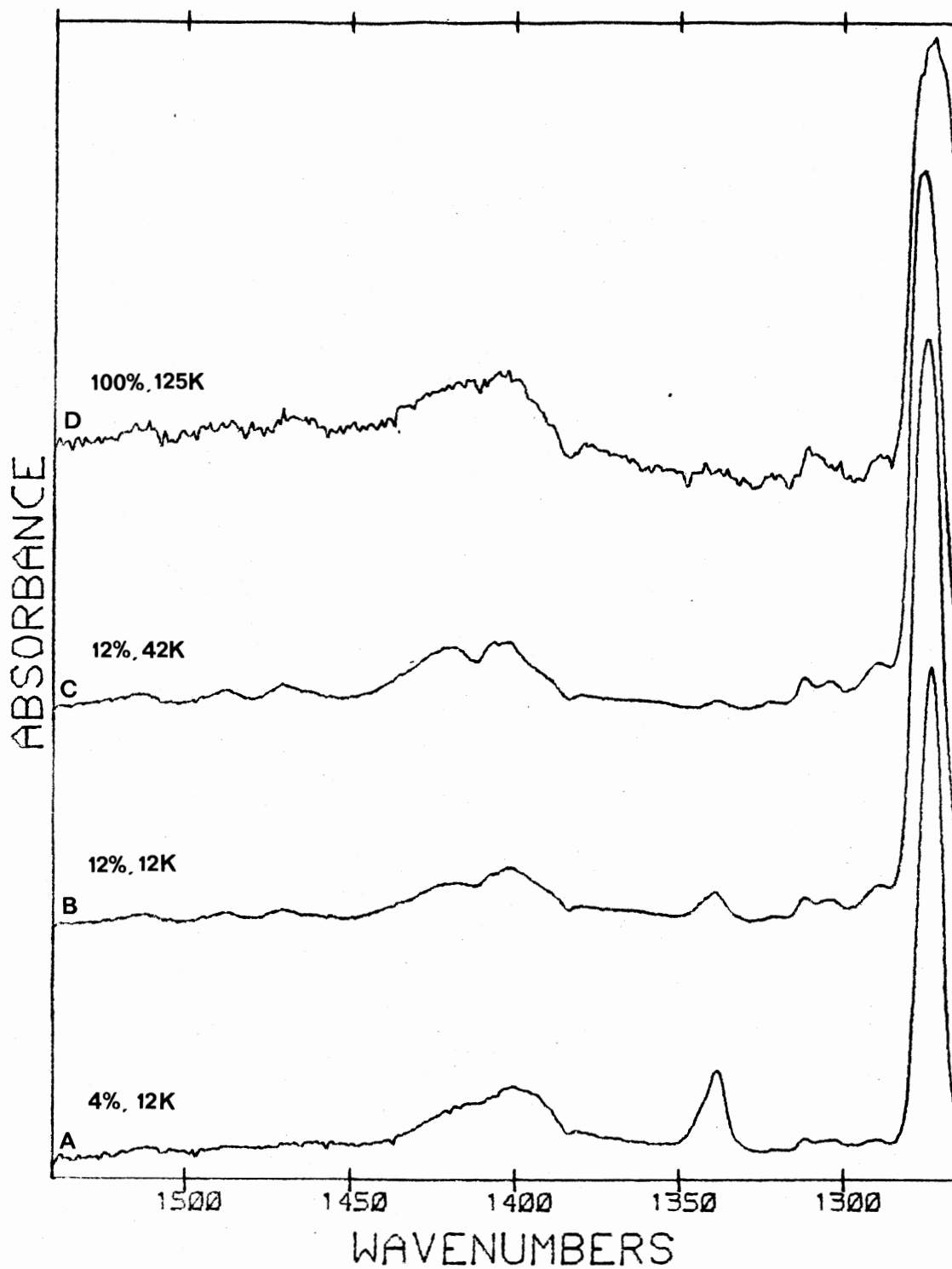


Figure 8. Matrix Spectra of t-Butanol
Isolated in Argon

visible in these spectra. These 4 steps are assigned to 4 cation solvates of the ion pair. Table 7 lists the band component locations for each of the spectra in Figure 7. The bands corresponding to the bare ion pair and the first solvate are sharp, but the second through fourth solvates are characterized by bands that become progressively broader as the solvent concentration in the matrix increases. This broadening of bands increases the difficulty of accurately determining the positions of these bands. As can be seen from Table 7, as the solvent concentration in the matrices increases, the ν_3 components of the higher solvates are shifted to lower frequency. This broadening and shifting is attributed to anion solvation, a behavior that is frequently observed in matrix spectra (22).

The maximum splittings of the nitrate ν_3 mode for each solvate are given in Table 8, along with the values for THF and H₂O solvates taken from reference (7). Table 9 lists the changes in the splitting of ν_3 for each of the solvation steps of the ion pairs. Included in the table for comparison is similar data for THF and H₂O taken from reference (7). The change in step size for the first two solvation steps for the t-butanol solvates are similar in magnitude to those of the THF solvates, and are also typical of the first three step sizes observed for the the smaller solvent molecule H₂O (7). Since any steric effect should be negligibly small for the first solvation step, and small for the second step, and since the change in step size for the

TABLE 7
 APPROXIMATE BAND POSITIONS FOR THE SPECTRA
 IN FIGURE 2

Spectrum, % Solvent and Temperature	Solvate Band Position, cm^{-1}							
	1		2		3		4	
	ν_{3a}	ν_{3b}	ν_{3a}	ν_{3b}	ν_{3a}	ν_{3b}	ν_{3a}	ν_{3b}
A, 1% at 9K	1514	1279	1494	1289				
B, 4% at 14K	1510		1490	1288				
C, 12% at 12K			1486	1289	1450	1312		
D, 12% at 42K			1478		1444	1314	1415	1340
E, 100% at 125K					1437		1409	1346

TABLE 8

FREQUENCY ASSIGNMENTS AND MAXIMUM SPLITTINGS FOR
THE CATION SOLVATES OF THE LITHIUM NITRATE ION
PAIR SOLVATED BY T-BUTANOL, AND A COMPARISON
WITH THE SPLITTINGS FOR THF AND H₂O

Solvate	-1 cm			-1 cm	
	v _{3a}	t-Butanol v _{3b}	Splitting	Splitting (Ref. 7) THF	H ₂ O
0	1529	1264	265	262	262
1	1514	1279	235	233	241
2	1494	1288	206	198	210
3	1450	1312	138	150	175
4	1415	1340	75	105	100
5	--	--	--	--	65

TABLE 9

A COMPARISON OF THE CHANGE IN SPLITTING OF v₃ FOR
EACH SOLVATION STEP IN THE SOLVATION OF
LITHIUM NITRATE ION PAIRS BY
T-BUTANOL, THF, AND H₂O

Step	-1 Change in Splitting, cm		
	t-Butanol	THF	H ₂ O
0 - 1	30	29	21
1 - 2	29	35	31
2 - 3	68	48	35
3 - 4	63	45	75
4 - 5	--	--	35

first two steps is relatively independent of the size of the solvent molecule, the collapse in ν_3 for the initial stages of solvation is attributed primarily to cation charge neutralization by the solvent molecules. However, for the third solvation step in both the t-butanol and THF cases, the change in splitting increases much more significantly than when smaller solvent molecules such as H₂O are used. The effect is especially dramatic for the t-butanol solvates, with the change in splitting more than doubling from the 1-2 to 2-3 solvation step. The greater change in splitting for the t-butanol case (68 cm⁻¹) relative to the THF case (48 cm⁻¹) is probably due to an enhancement of the steric effect due to the greater size of the t-butanol molecule. In addition, the residual splitting of ν_3 for the highest solvate (the 4-solvate) is much smaller in the t-butanol case (63 cm⁻¹), as compared to approximately 100 cm⁻¹ in THF, adding to the evidence for an enhanced steric effect with t-butanol.

Any judgment as to whether a switch from bidentate binding to monodentate binding occurs for the 2-3 solvation step with t-butanol is not conclusive. An attempt by other workers in this lab to determine Raman depolarization ratios for liquid t-butanol/LiNO₃ was unsuccessful since LiNO₃ was found to be only slightly soluble in t-butanol, a fact which made Raman spectra of sufficient intensity impossible to obtain. It is possible that the large change in splitting of ν_3 observed for the 2-3 solvation step is due in part to

a change in binding. An observation of space-filling models for this system reveals the high degree of steric crowding present in the inner-coordination sphere of the ion pair. Based on this observation it seems unlikely that four t-butanol molecules could fit into the inner-coordination sphere of the Li^+ ion without a change in binding from bidentate to monodentate occurring at some stage of solvation.

Figure 9 illustrates the effect a change in cation has on the splitting of ν_3 . Spectrum (A) is K^+NO_3^- isolated in 100% t-butanol at 90 K, while spectrum (B) is Li^+NO_3^- isolated in 100% t-butanol at 90 K. As can be seen from the spectra, a difference in cation has a definite effect on the splitting of ν_3 , indicating that contact pairing between the cation and anion is retained at this stage of solvation in the matrix samples. The splitting of the highest observed solvate of K^+NO_3^- is 48 cm^{-1} , while that for Li^+NO_3^- is approximately 65 cm^{-1} . The larger splitting for the Li^+NO_3^- case is indicative of the greater ability of the Li^+ ion to perturb the contacting NO_3^- ion due to the greater charge density of the smaller Li^+ ion (21).

Figure 10 is of the spectra in Figure 9 after annealing to 160 K. The splitting for K^+NO_3^- after annealing (spectrum A) is 48 cm^{-1} while the splitting for Li^+NO_3^- (spectrum B) is 55 cm^{-1} , yielding a difference in splitting of approximately 7 cm^{-1} . A cation dependence is still present indicating that the cation and anion are likely

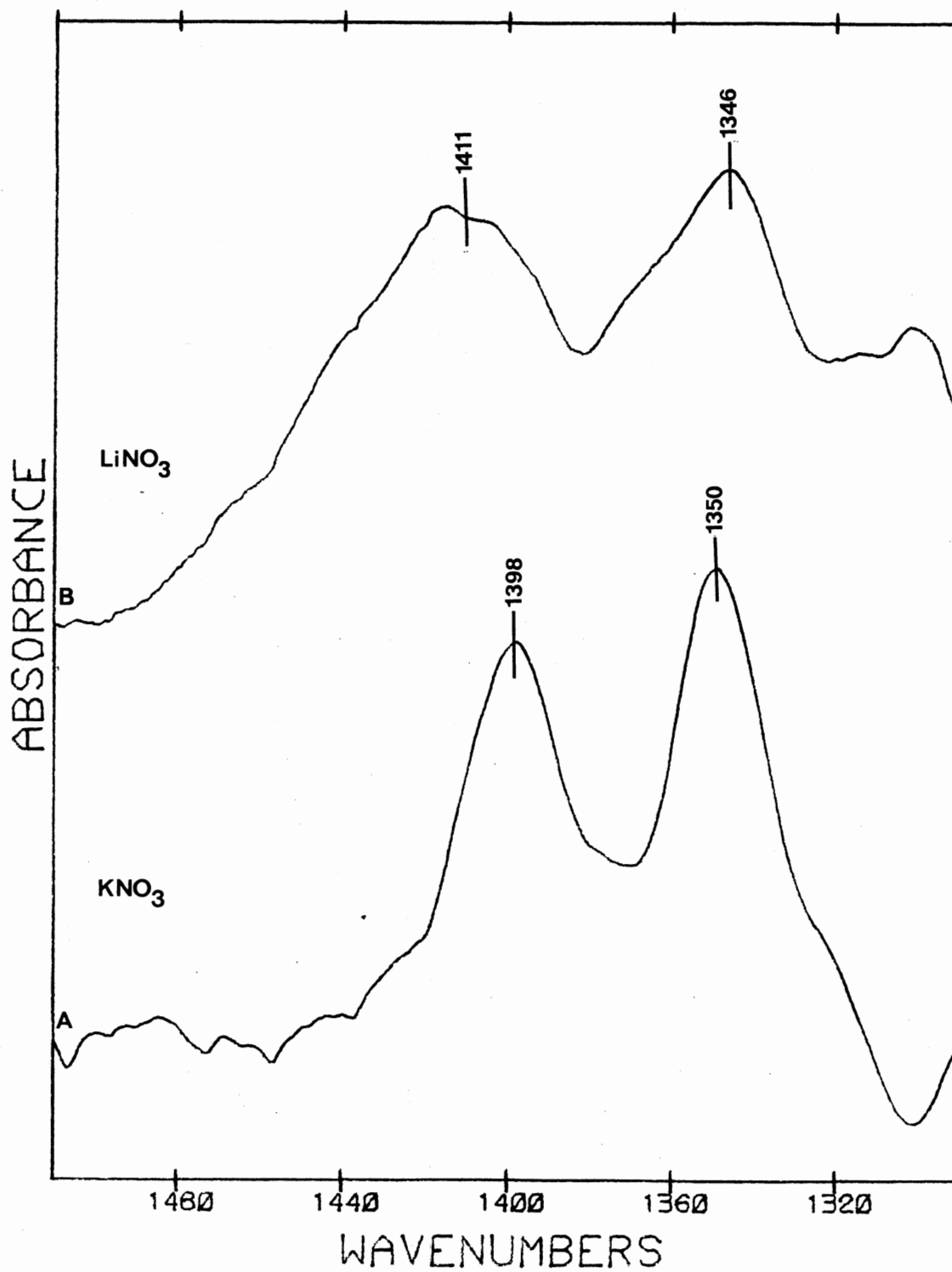


Figure 9. Infrared Spectra of 90 K Deposits of K^+NO_3^- and Li^+NO_3^- in Pure t-Butanol

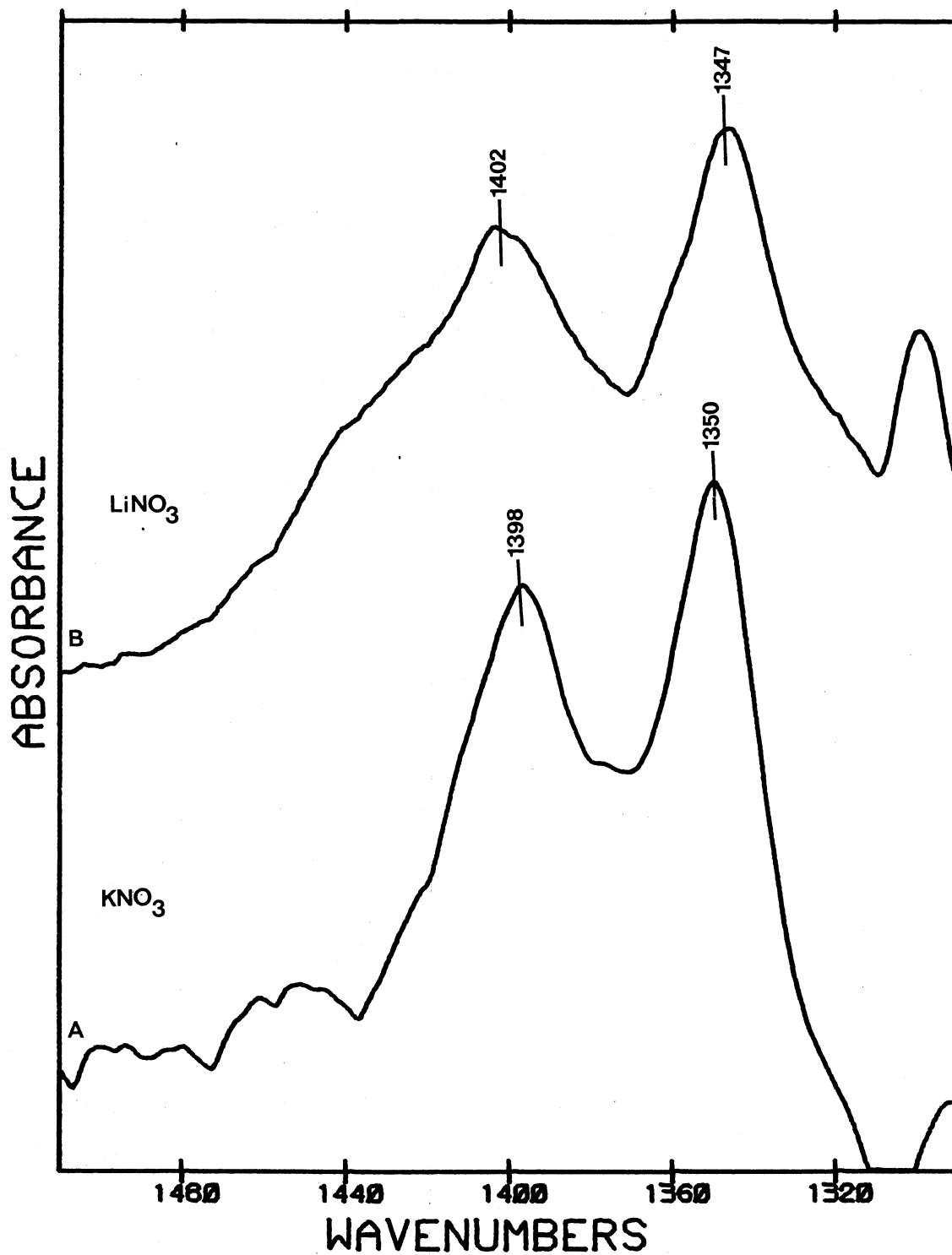


Figure 10. Infrared Spectra of 90 K Deposits of K+NO₃ and Li+NO₃⁻ in Pure t-Butanol after Annealing to 160 K

contact paired. Of interest is the change in band positions for Li^+NO_3^- after annealing. The splitting has collapsed from approximately 65 cm^{-1} to 55 cm^{-1} upon annealing for Li^+NO_3^- , while the band positions are relatively unchanged for the K^+NO_3^- case. Since a cation effect is observable, it is doubtful that solvent insertion is responsible for the further collapse in the splitting for Li^+NO_3^- . It is possible that an increase in anion solvation upon annealing is responsible for the shift, but it seems odd that the effect would be noticed only for Li^+NO_3^- . Another possibility is that the 4-solvate is not the maximum solvate for Li^+NO_3^- in t-butanol, and the further collapse in ν_3 is due to the formation of a higher solvate. Since t-butanol will hydrogen-bond with the nitrate ion, perturbation of the nitrate ion through hydrogen bonding will result in a splitting of ν_3 , eliminating the possibility of observing any distortion of the anion by the cation that would produce a splitting less than that due to anion solvation. An attempt to determine the splitting of ν_3 of solvated (free) nitrate ion in dilute solutions of liquid t-butanol was unsuccessful due to the fact that alkali-metal nitrate salts, as already mentioned, are fairly insoluble in t-butanol. A value of 66 cm^{-1} has been reported by Findlay (35) for the splitting of ν_3 due to solvation of the nitrate ion by methanol in dilute room-temperature solutions of NaNO_3 in methanol. The strength of the hydrogen-bonding in t-butanol solutions would not be expected to be as strong as

in a methanol solution, so the limiting value for the splitting in t-butanol solutions would be less than the value reported for methanol. From this study, the value for the splitting of ν_3 due to anion solvation by t-butanol would be less than or equal to 48 cm^{-1} , which is the minimum splitting observed for K^+NO_3^- . In the K^+NO_3^- case it is possible that solvent insertion has occurred before annealing, and the residual splitting observed is due mainly to anion solvation. This may account for the fact that the K^+NO_3^- spectrum did not change appreciably upon annealing. In either case, the data is inconclusive and any firm judgments as to the cause of the effects are difficult to make.

Figure 11 illustrates the effect of deposition temperature and annealing on the spectra of Li^+NO_3^- in pure t-butanol. Spectrum (A) is of a 16 K deposit. At 16 K, the 3-solvate dominates the spectrum, with almost as much of the 2-solvate present as the 4-solvate. Spectra (B) and (C) show the same sample after annealing to 100 K and 125 K respectively. The 4-solvate dominates the spectrum after annealing, but the 3-solvate is still visible in both spectra. Spectrum (D), a different sample deposited at 90 K, is dominated by the 4-solvate. Figure 12 is another sample of Li^+NO_3^- ion pairs isolated in pure t-butanol at 90 K (spectrum A), followed by annealing to 160 K (spectrum B) and to 180 K (spectrum C). Only after this rather extreme annealing do the ν_3 band components for the 3-solvate

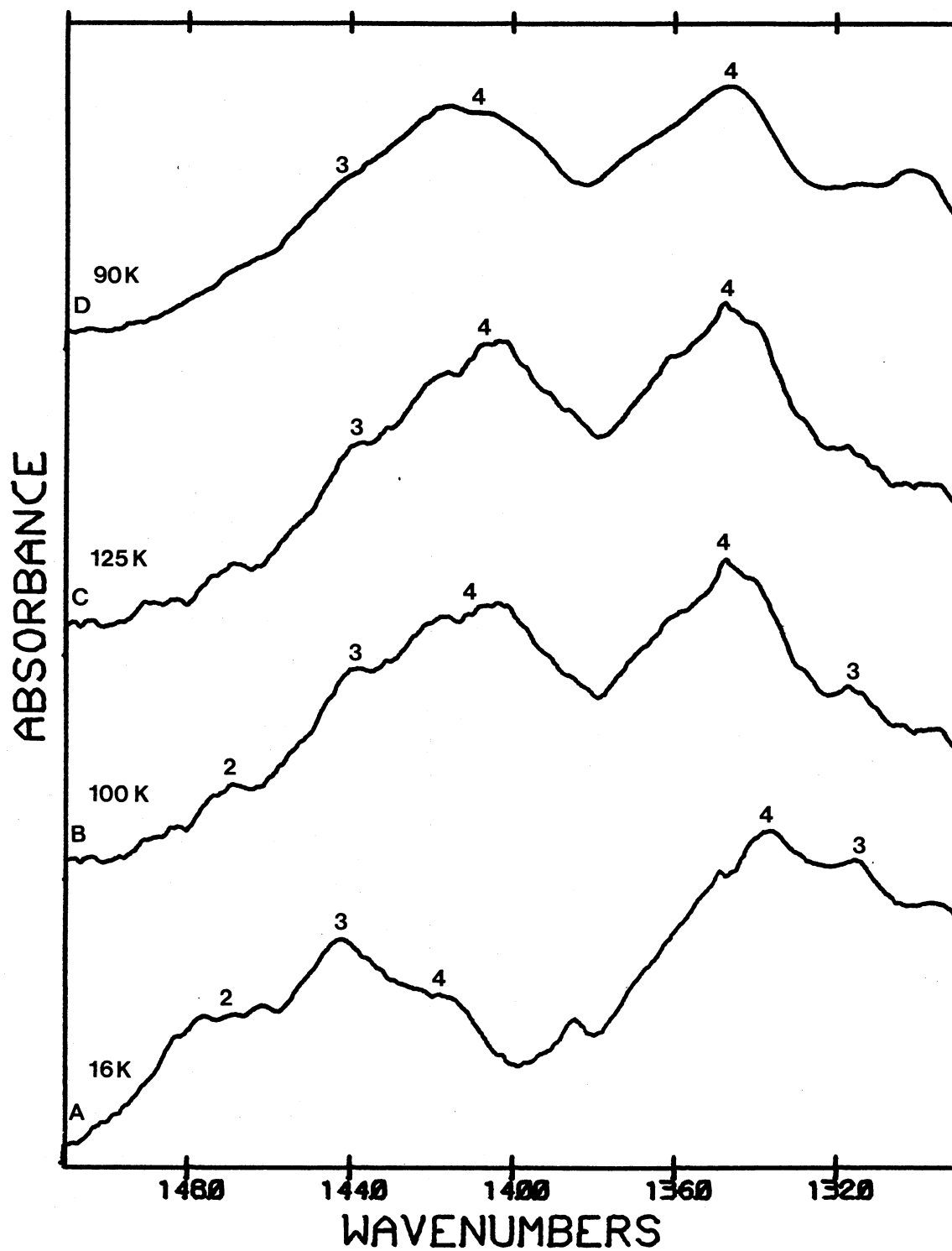


Figure 11. The Effect of Deposition Temperature and Annealing on the Infrared Spectra of the Solvates of Li^+NO_3^- Matrix Isolated in Pure *t*-Butanol

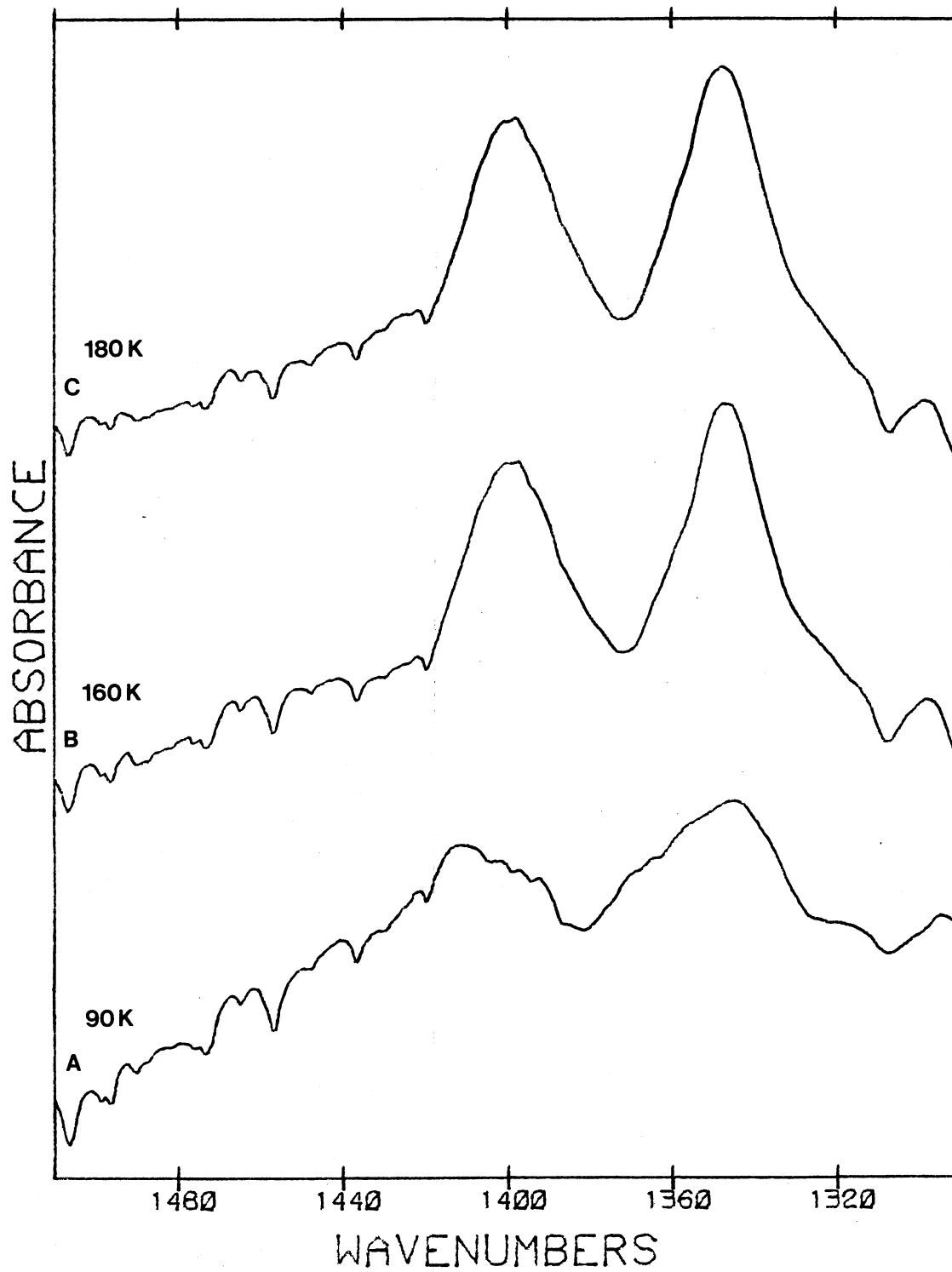


Figure 12. The Effect of Annealing on the Matrix Spectra of Li^+NO_3^- Ion Pairs Isolated in Pure *t*-Butanol

completely disappear.

The presence of lower solvates in pure solvent matrices at low temperatures (12 K - 16 K) is common, but the degree of kinetic stabilization in this case is unusual. Figure 13 illustrates this high degree of stabilization. Spectrum (A) of Figure 13 is of Li^+NO_3^- in pure t-butanol at 12 K, and spectrum (B) is of Li^+NO_3^- in pure H_2O at 14 K. In the case of t-butanol, the lower solvates (the 2 and 3-solvates) dominate the spectrum, while in the case of H_2O the highest solvate (the 5-solvate) dominates the spectrum. Data from liquid solutions of LiNO_3 and t-butanol indicate that ion-pair solvation is an exothermic process for the 3 to 4 solvation step in t-butanol (33). This finding suggests that lower temperatures should favor the formation of the higher solvates. Thus, it is unlikely that an equilibrium liquid solution of t-butanol and LiNO_3 at 16 K (impossible in this case) would contain the high concentrations of the 2 and 3 solvates present in the matrix samples. A possible explanation for the high concentration of the lower solvates in the matrix samples is that the bulky t-butanol molecules are having difficulty achieving the proper orientation for solvation in the low-temperature matrix samples (33). At higher temperatures (the annealed samples), the sample contains a sufficient amount of energy to enable diffusion in the matrix, giving the solvent molecules an enhanced probability of achieving the proper orientation for solvation. Thus, upon annealing the sample a reduction in

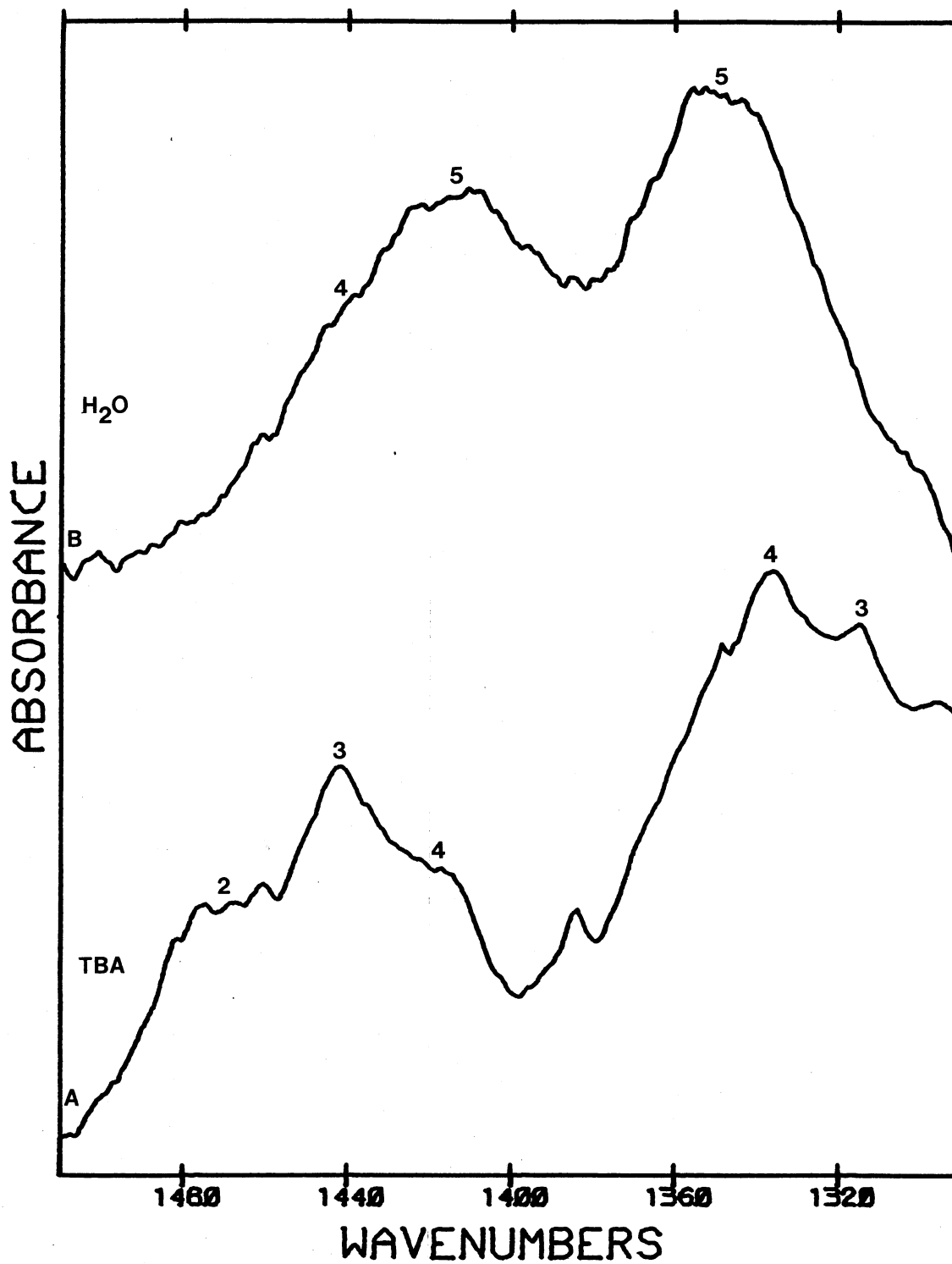


Figure 13. A Comparison of Minimum Temperature Deposits of Li^+NO_3^- Ion Pairs in Pure Water and Pure t-Butanol

the concentration of the lower solvates is observed. From Figure 12 it can also be noted that the band components for ν_3 become sharper and more well-defined upon annealing. This would indicate that at higher temperatures the solvent is more successful in achieving the proper orientation for solvation leading to a more well-defined and specific solvate structure (22) which results in a sharpening of the band components of ν_3 .

An additional observation from Figure 11 can be made upon comparison of spectrum (A) with spectrum (D). Assuming the the matrix remains rigid during deposition at 90 K, it seems odd that none of the 2-solvate and little of the 3-solvate is visible in spectrum (D), while both the 2 and 3-solvates are plainly visible in the 16 K deposit (spectrum A). A possible explanation is that the surface of a matrix deposited at 90 K possesses a much higher degree of fluidity than does the surface of a 16 K deposit. This fluidity at the matrix surface as the sample forms would result in an enhanced probability of solvent molecules seeking out ion pairs and achieving the proper orientation for solvation before the surface layer of the matrix becomes rigid as it is incorporated into the bulk of the matrix as the sample grows.

Results for Water as Solvent

The matrix solvation spectra for the hydrates of Li^+NO_3^- have been reported previously by Ritzhaupt and

co-workers (7). Their results show 5 clearly defined solvation stages which have previously been assigned to 5 distinct cation hydrates.

Since water is a dissociating solvent, there has been some question as to whether the final stages of ion-pair hydration in pure water matrices results in solvent separated ions rather than contact ion pairs. Part of the work done in the present study was an attempt to determine if varying the degree of fluidity at the surface of a growing matrix influenced the nature of the cation - anion interaction observed in the latter stages of ion-pair solvation in pure water matrices.

Figure 14 illustrates the effect of varying deposition temperature on the matrix-solvation spectra for Li^+NO_3^- in pure water matrices. Spectrum (A) is for a 12 K deposit while spectra (B) and (C) are for two different 90 K deposits. As can be seen from Figure 14, the splittings vary, with the splitting ranging from a value of 65 cm^{-1} for the 12 K deposit (spectrum A) to 58 cm^{-1} for one of the 90 K deposits (spectrum C). Of particular interest is the shoulder denoted by a dashed line in spectrum (A) and in spectrum (B). This shoulder could be detected in all the 12 K samples and in about 25% of the samples prepared at 90 K. Spectrum (B) is representative of the data collected for 90 K deposits in which the shoulder was very weak but visible, and spectrum (C) is representative of the samples in which the shoulder was absent. Upon annealing to 120 K,

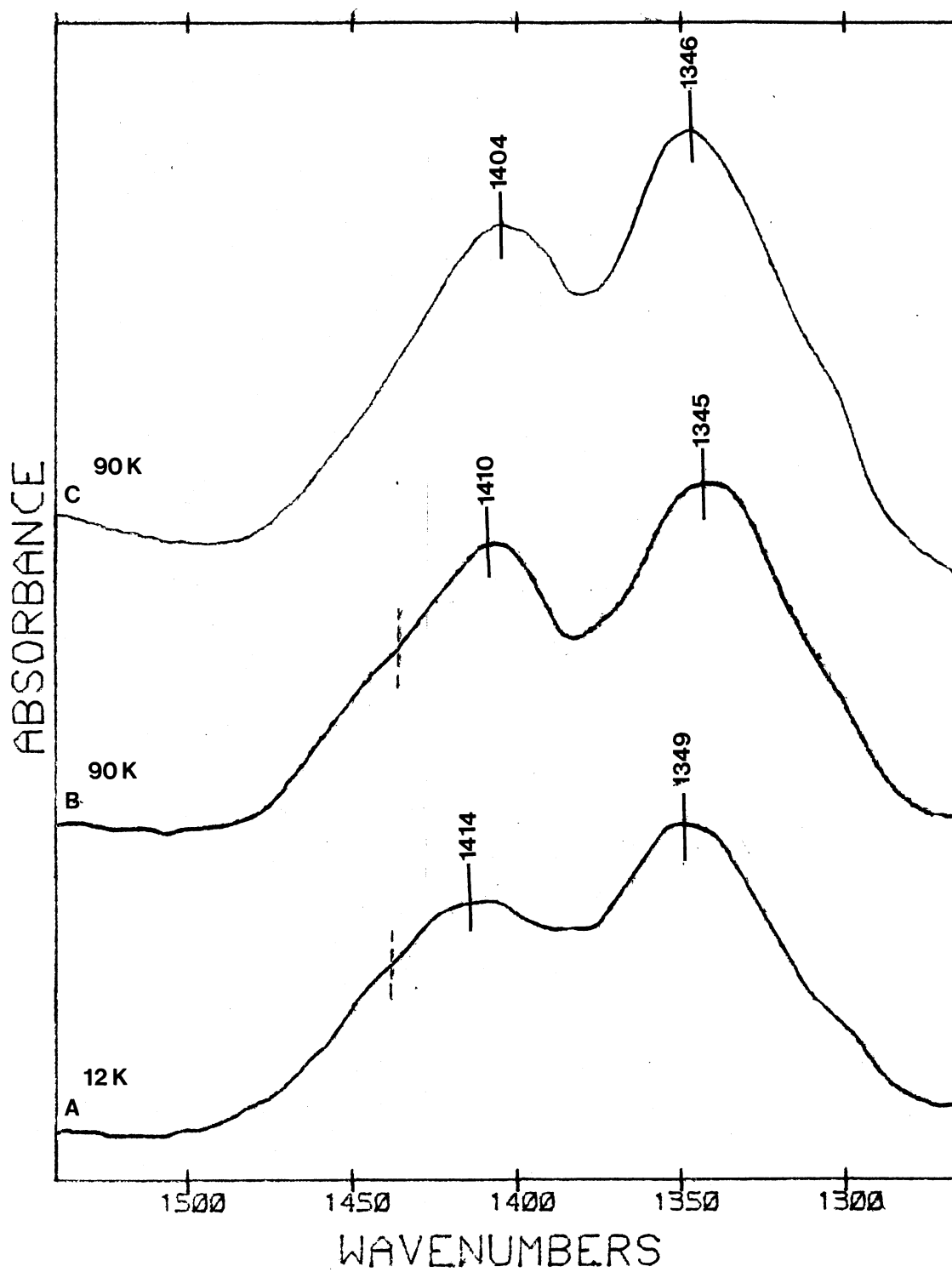


Figure 14. The Effect of Deposition Temperature on the Matrix-Hydration Spectra of Li^+NO_3^- Ion Pairs in Pure Water Matrices

the shoulders in spectra (A) and (B) disappear and the splitting collapses yielding spectra very similar to spectrum (C). The position of the shoulder in these spectra (approximately 1440 cm^{-1}) closely matches the 1437 cm^{-1} position of ν_{3a} for the 4-hydrate of Li^+NO_3^- reported by Ritzhaupt (7). Because of the similarity in the positions of ν_{3a} for the 4-hydrate and the shoulder, and due to the fact that the shoulder disappears upon annealing, the shoulder in spectrum (A) and in spectrum (B) is assigned to the 4-hydrate of Li^+NO_3^- . Following this assignment, the minimum temperature deposit is probably a mixture of the 4 and 5 hydrates while the 90 K deposits consist largely of the 5-hydrate. A possible explanation for this is that increased fluidity at the matrix surface at 90 K enhances the probability of hydration before the surface layer of the matrix becomes rigid as it is incorporated into the bulk of the matrix, hence favoring formation of the more stable 5-hydrate over the 4-hydrate.

Figure 15 depicts the effect a change in cation has upon the spectra for the maximum observable hydrates of a series of alkali-metal nitrates prepared at 90 K in pure water matrices. Spectrum (A) is for Rb^+NO_3^- , spectrum (B) is for K^+NO_3^- , and spectrum (C) is for Li^+NO_3^- . The splitting observed for the Rb^+NO_3^- hydrate is 50 cm^{-1} , 52 cm^{-1} for the K^+NO_3^- hydrate, and 58 cm^{-1} for Li^+NO_3^- hydrate. A small cation effect is observable, with the magnitude of the splitting increasing as the polarizing

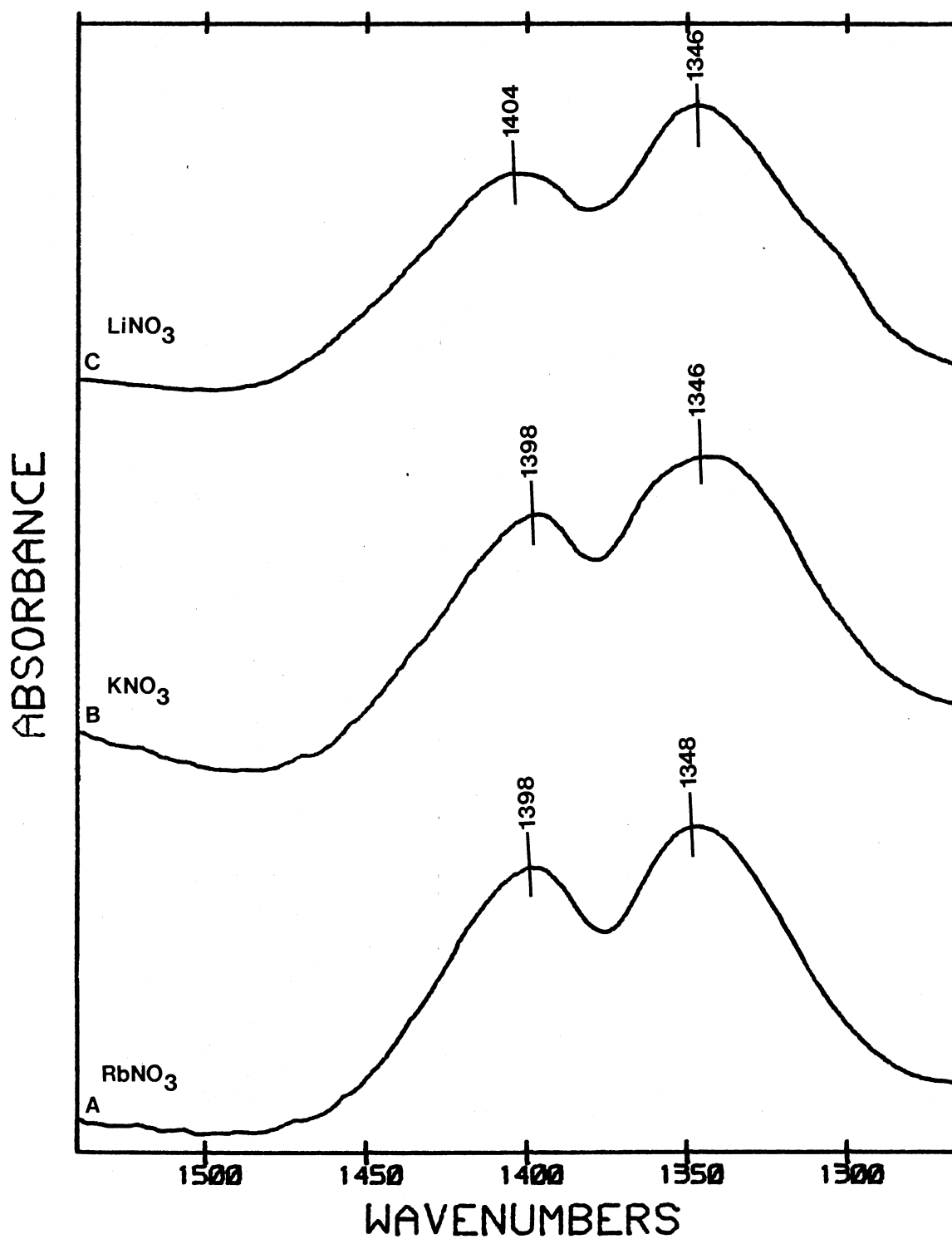


Figure 15. The Effect of a Change in Cation on the Matrix Hydration Spectra of Alkali-Metal Nitrate Ion Pairs in Pure Water Matrices

power of the cation increases. Li^+ , which has the smallest size and hence greatest charge density and polarizing ability of the three cations, has the greatest effect on the splitting of ν_3 . The decrease in splitting observed when changing from K^+ to Rb^+ is small (approximately 2 cm^{-1}), making these measurements the same within the limits of experimental error. There was little or no observable effect on these spectra after annealing.

Whether or not solvent insertion has occurred for the 5-hydrate of Li^+NO_3^- in pure water matrices is still uncertain. The fact that a cation effect is still visible for the maximum observable hydrates would indicate that contact pairing is probably retained at this stage of solvation in the matrices, especially for Li^+NO_3^- . Since water strongly perturbs the nitrate ion through hydrogen bonding, it is impossible to observe any ion pair hydrates (or solvent-separated ions) that might produce a splitting of less than that resulting from nitrate ion solvation by water. In dilute, aqueous, alkali-metal nitrate solutions at room temperature, a splitting of approximately 48 cm^{-1} is observed and has been attributed to solvation of the free nitrate ion by water (11). It is assumed in this work that a similar value for the splitting due to anion solvation is observed in matrices, implying that any perturbation of the anion resulting in a splitting of less than approximately 50 cm^{-1} is impossible to observe. It is difficult to conceive that a solvent-separated ion pair would produce a splitting

less than that due to hydration of the free anion. This new data does not contradict any previous findings, but does little to clarify details concerning the later stages of ion pair hydration in matrices.

In light of the finding that the degree of fluidity present at the growing surface of a matrix has a definite effect on nature of the species trapped from the vapor phase may weakly support Mayer's conclusions regarding vitrification of dilute aqueous solutions of alkali-metal nitrates and perchlorates (34). Since these solutions should largely consist of completely solvated ions, the spectra of these samples formed by rapidly cooling aerosol droplets onto a cryoplate should indicate the presence of mostly free ions if the aerosol is quenched rapidly enough to eliminate any restructuring of the liquid solution structure. As previously discussed, Mayer reports that vitrification of dilute aqueous LiNO_3 solutions using this technique results in contact-paired hydrates, while for KNO_3 and RbNO_3 solvent separated ion pairs result. The spectrum published by Mayer for the LiNO_3 solution very closely resembles the spectrum of the matrix-isolated hydrates of contact-paired LiNO_3 presented in this work.

The results of Mayer would indicate that a decrease in temperature favors ion pairing, a finding which is, as previously mentioned, inconsistent with an increasing amount of data that would indicate the opposite is true (36) (13). Fluidity at the surface of a growing matrix may enable the

formation of contact ion pairs and solvent-separated ion pairs before the matrix becomes rigid, if indeed ion-pairing is favored by a decrease in temperature.

A possibility which cannot be overlooked in Mayer's data is that freeze-concentration of the solution may be occurring because of localized crystallization of the solution upon quenching. Any increase in the concentration of the solution could lead to ion pairing. Since amorphous water is in a metastable state, crystallization of the water in the sample will occur if precautions are not taken to prevent it. Due to the rapid rate of deposition used by Mayer (10 to 25 seconds was sufficient to obtain a sample of adequate thickness as compared to 2 to 6 hours for the matrix samples in this study), it is quite possible that the cooling rate of the sample was not adequate to prevent a degree of crystallization in the sample.

Summary

The effect of steric crowding on matrix solvation spectra was studied using t-butanol, the bulkiest deuterated solvent commercially available. The first two solvation steps of Li^+NO_3^- resulted in changes in splitting of the nitrate vs mode similar to those produced when smaller solvent molecules such as water (7) were used. An unusually large change in the splitting for the third solvation step was observed. This unusually large step size was attributed to an increased steric effect due to the large size of the

t-butanol molecule. It has been anticipated that at some stage of solvation the binding between alkali-metal cations and the nitrate ion, which has been shown to be bidentate in nature (8) (9) (10) (23) (24) (25), would switch to monodentate to reduce steric crowding within the solvation sphere of the ion pair, resulting in a lower energy, and thus more stable, configuration. A firm conclusion as to whether a change in binding occurred during the third solvation step using t-butanol could not be made. The large increase in step size for the third solvation step could be due in part to a change in binding (22) (26).

The effect of matrix fluidity on matrix-solvation spectra was also investigated. A definite effect was observed, with higher deposition temperatures favoring the formation of higher solvates for both t-butanol and water solvents. The higher degree of fluidity present in the higher temperature deposits increases the probability of solvation by allowing the solvent molecules and ion pairs to more easily achieve the proper orientations for solvation before becoming trapped as the matrix becomes rigid. This finding increases the concern that solvent insertion could occur in the latter stages of matrix solvation when dissociating solvents such as water are used. No new evidence was found to firmly support or disprove that solvent insertion was responsible for the final solvation step of Li^+NO_3^- ion pairs in pure water matrices (7). The finding that matrix fluidity has a definite effect on the

species trapped from the vapor phase may weakly support the claims of Mayer (34) that vitrification of dilute aqueous solutions of LiNO_3 result in the formation of mostly contact ion pairs while vitrification of dilute solutions of KNO_3 and RbNO_3 result in mostly solvent-separated ion pairs.

REFERENCES

1. Fuoss, R. M., and Accascina, F., Electrolytic Conductance, Interscience Publishers, New York, 1959.
2. Nancollas, G. H., Interactions In Electrolyte Solutions, Elsevier Publishing Co., New York, 1966.
3. Debye, P., and Huckel, E., *Z. Physik*, 25, 97, (1924).
4. Irish, D. E., in Ionic Interactions From Dilute Solutions to Fused Salts, vol. 2, Petrucci, E., ed., Academic Press, New York, 1971.
5. Conway, B. E., Ionic Hydration in Chemistry and Biophysics, Elsevier Publishing Co., New York, 1981.
6. Toth, J. P., Ritzhaupt, G. R., and Devlin, J. P., *J. Phys. Chem.*, 85, 1387, (1981).
7. Ritzhaupt, G., Consani, K., and Devlin, J. P., *J. Chem. Phys.*, 82, 1167, (1985).
8. Beattie, I. R., Ogden, J. S., and Price, D. D., *J. Chem. Soc. Dalton Trans.*, 16, 1460, (1979).
9. Bencivenni, D., and Gingerich, K. A., *J. Molec. Struc.*, 98, 195, (1983).
10. Moore, J. C., and Devlin, J. P., *J. Chem. Phys.*, 68, 826, (1978).
11. Irish, D. E., and Davis, A. R., *Can. J. Chem.*, 46, 943, (1968).
12. Heinje, G., Luck, W. A. P., and Heinzinger, K., *J. Phys. Chem.*, 91, 331, (1987).
13. Wooldridge, R., Fisher, M., Ritzhaupt, G., and Devlin, J. P., *J. Chem. Phys.*, 86, 4391, (1987).
14. Edgell, W. F., and Harris, D., *J. Soln. Chem.*, 9, 649, (1980).

15. Devlin, J. P., in Vibrational Spectra and Structure, vol. 16, Durig, J. R., ed., Elsevier Science Publishing Co., New York, (1987).
16. Bauer, S. H., and Porter, R. F., in Molten Salt Chemistry, Blander, M., ed., Interscience Publishers, Inc., New York, (1964).
17. Buchler, A., and Stauffer, J. L., *J. Phys. Chem.*, 70, 4092, (1966).
18. Smith, D., James, D. W., and Devlin, J. P., *J. Chem. Phys.*, 54, 4437, (1971).
19. Craddock, S., and Hinchcliffe, A. J., Matrix Isolation, Cambridge University Press, London, (1975).
20. Janz, G. J., and Kozlowski, T. R., *J. Chem. Phys.*, 40, 1699, (1964).
21. Smyrl, N., and Devlin, J. P., *J. Phys. Chem.*, 77, 3067, (1973).
22. Devlin, J. P., and Consani, K., *J. Phys. Chem.*, 88, 3269, (1984).
23. Beattie, I. R., and Parkinson, J. E., *J. Chem. Soc. Dalton Trans.*, 1363, (1984).
24. Ritzhaupt, G., and Devlin, J. P., *J. Chem. Phys.*, 62, 1982, (1975).
25. Ritzhaupt, G., Richardson, H., and Devlin, J. P., *High Temp. Sci.*, 19, 163, (1985).
26. Hester, R. E., and Grossman, W. E. L., *Inorg. Chem.*, 5, 1308, (1966).
27. Brintzinger, H., and Hester, R. E., *Inorg. Chem.*, 5, 980, (1966).
28. Colthup, N., Daly, L., and Wiberly, S., Introduction to Infrared and Raman Spectroscopy, Academic Press, New York, (1975).
29. Khodchenkov, A. N., Spiridonov, V. P., and Akiskin, P. A., *Zh. Strukt. Khim.*, 6, 724, (1965).
30. Castelman, A. W., Holland, P. M., Lindsay, D., and Peterson, K., *J. Am. Chem. Soc.*, 100, 6039, (1978).

31. Ritzhaupt, G., and Devlin, J. P., J. Phys. Chem., 79, 2265, (1975).
32. Mayes, R. E., and James, D. W., unpublished results.
33. Devlin, J. P., Ritzhaupt, G., Fisher, M., and Wooldridge, R., Faraday Discuss. Chem. Soc., 85, 255, (1988).
34. Mayer, E., J. Phys. Chem., 90, 4455, (1986).
35. Findlay, T. J. V., and Symons, M. C. R., J. Chem. Soc. Faraday Trans. 1, 72, 820, (1976).
36. Guillaume, F., and Rothschild, W. G., J. Chem. Phys., 83, 4338, (1985).

7
VITA

Mark Edwin Fisher

Candidate for the Degree of
Master of Science

Thesis: A SPECTROSCOPIC STUDY OF IONIC SOLVATION: THE
EFFECTS OF STERIC CROWDING AND MATRIX FLUIDITY ON
MATRIX SOLVATION SPECTRA

Major Field: Chemistry

Biographical:

Personal Data: Born in Frederick, Oklahoma on May 10,
1962, one of three children of Carl E. and Elwana
L. Fisher.

Education: Graduated from Chattanooga High School,
Chattanooga, Oklahoma, in 1980; received Bachelor
of Science degree from Cameron University, Lawton,
Oklahoma with a major in Chemistry and a minor in
Mathematics, in May 1985; and completed the
requirements for the Master of Science degree at
Oklahoma State University, July, 1989.

Professional Experience: Graduate Teaching Assistant:
Fall, 1985 - Spring, 1987; 1988; Spring, 1989.
Graduate Research Assistant: Summer, 1986; Summer,
1987; Fall, 1987; Summer, 1988; Spring, 1989;
Summer, 1989.